Inorganic nanoparticles as potential regulators of immune response in dendritic cells

Nanomedicine

Inorganic Nanoparticles as Potential Regulators of Immune Response in Dendritic Cells

Journal:	*Nanomedicine*
Manuscript ID	NNM-2017-0061
Manuscript Type:	Research Article
Keywords:	Nanoparticles, Protein Corona, Cancer Immunotherapy

Inorganic Nanoparticles as Potential Regulators of Immune Response in Dendritic Cells

STRUCTURED ABSTRACT:

Aim: The spontaneous adsorption of proteins on nanoparticles (NPs) in biological media is exploited to prepare association complexes of NPs and proteins from cancer cells' lysates for application in cancer immunotherapy. **Materials & methods:** gold and silica NPs were synthesized, incubated with cancer cells' lysates and characterized from a compositional and physico-chemical point of view. Immature Dendritic Cells (DC) were challenged with the protein-coated NPs and their maturation profiles, viability and morphology were evaluated. Finally, lymphocytes T proliferation was determined. **Results & conclusions:** silica and gold NPs bind different pools of biomolecules from the same lysates, opening the possibility to be used as selective carriers for antigens. When incubated with immature DCs, NPs were efficiently endocyted without cytotoxic effects. Finally, AuNPs promoted DC maturation and DC-mediated lymphocyte proliferation, at variance with SiO_2NPs. Overall, these results demonstrate that the spontaneous formation of different protein *coronas* on different NPs represents a possible approach to fast, easy, cost-effective DC stimulation tools, that may eventually become of use for cancer immunotherapy.

KEYWORDS: Nanoparticles; Protein Corona; Cancer Immunotherapy

INTRODUCTION

In spite of the intense efforts and progresses of medical research, the treatment of tumors still represents an open challenge. A relatively recent and promising approach for cancer therapy is based on the stimulation of the immune system of the patient itself against the tumor, thus adopting a vaccination strategy for tumor treatment [1]. Because of the immune system's extraordinary

power, its capacity for memory, its exquisite specificity, and its central and universal role in human biology, cancer immunotherapy has the potential to achieve complete, long-lasting remissions and cancer cure, with few or no side effects, and for any cancer patient, regardless of cancer type. However, while the basic concept of cancer immunotherapy can appear straightforward, its translation into medical application is still far to reach, due to several open challenges. A main role in cancer immunotherapy is played by dendritic cells (DCs), that possess intrinsic antigen-presenting properties to elicit a potent tumor antigen-specific T-cell-driven immune response [2-4]. The efficient delivery of tumor antigens to immature DCs, recognition of antigens by these cells and induction of DC maturation are key steps of the entire process. However, many hurdles have to be overcome to obtain the desired immune response. In fact, not only the antigen must be recognized by the DCs, but the maturation of a correct subset of those cells must be induced [5] and the mature DCs have to trigger the differentiation of antigen-specific T cells into effector T cells able to exert anti-cancer cytotoxicity [6].

The use of nanomaterials has been recently presented in a few studies on cancer immunotherapy; mainly organic and biodegradable NPs have been used [7,8], but some inorganic materials have also been tested [9]. These systems have been used for several purposes, from the study of nanoparticles internalization in dendritic cells [10] to the delivery of antigens [7, 11]. However, a sophisticated methodology is often required to synthesize NPs and, in particular, to conjugate them with a specific antigen that has to be first of all selected, and then modified or even synthesized [12,13]. In this work we present a new and simpler approach to nanoparticle-based antigen delivery.

Silica and gold NPs (SiO_2NPs and AuNPs) are among the most investigated nanodevices for biomedical applications. Both types of nanoparticles are characterized by well-established and easy-to-follow synthetic routes, high biocompatibility and tunable physicochemical properties (size, charge, shape). Due to the high surface energy of NPs, determined by the high surface/volume ratio [14-16], when they are dispersed in a biological medium, biomolecules, mostly proteins but also

nucleic acids and lipids, are adsorbed on the surface of NPs forming a so-called protein corona [7,14-16]. The protein corona is a dynamic system, that changes its composition constantly [15,16] and can be seen as an integral part of the nanosystem [17]. It is formed by a wide variety of biomolecules, some bound tightly to NP surface, forming the hard corona, others loosely bound and constituting the soft corona. While the hard corona follows the NP through all the biological events [14], the biomolecules in the soft corona continually exchange with other proteins in solution [15,16]. The NPs' physicochemical features, such as composition, surface charge and size [16,18], deeply influence the nature of their protein corona, whose composition in turn provides the physiological identity of NPs [19,20], being it what cells "see" and come in contact with. The influence that this protein layer has on the bioactivity of nanostructures is one of the most most addressed topics in nanomedicine [14].

In this work we have exploited the spontaneous formation of lysate coronas on NPs to build-up nanoparticle-based carriers for cancer immunotherapy applications. The simplest biocompatible, easily synthesized and common NP types, i.e. AuNPs and SiO_2NPs, were prepared according to Turkevich-Frens [21,22] and Stober [23] methods, respectively and characterized through Dynamic light scattering (DLS), transmission electron microscopy (TEM) and zeta potential. The NPs were exposed to two different types of whole cancer cell lysates, a hepatic (Hep G2) and an ovarian (A2780) cancer cell line. The lysates were obtained from whole cells and the protein corona was characterized through DLS, circular dichroism (CD) and mass spectrometry to determine their thickness and composition for each NP and cells' lysate type. Biological studies on the interaction of the two types of NPs with immature DCs were performed to evaluate the cells' internalization efficiency and possible cytotoxic effects. Finally, the effects of the NPs on the maturation of immature DCs and on DCs-mediated lymphocyte proliferation were investigated.

MATERIALS & METHODS

Chemicals and culture media

NPs Syntheses: Tetraethylorthosilicate (TEOS; 98%), 3-aminopropyl triethoxysilane, citric acid and rhodamine B isothiocyanate were purchased from Sigma-Aldrich (St. Louis, MO). Ethanol (>99.8%) and chloroauric acid were acquired from Fluka (Buchs, Switzerland). Ammonia (30%) was bought from Panreac (Castellar del Vallès, Spain). High-purity deionized water (18.2 MΩcm) was produced using A10 Milli-Q (Millipore, Darmstadt, Germany) and was used in all preparations. Dialysis tubing cellulose membranes (14,000 Da) were acquired from Sigma-Aldrich. **Cell culture:** Dulbecco's phosphate buffered saline was from EuroClone (Milan, Italy). Ficoll/Paque were from GE Healthcare (Little Chalfont, UK). RPMI 1640, heat-inactivated foetal bovine serum (FBS), penicillin, streptomycin and trypan blue were from Sigma-Aldrich. Immunomagnetic separation was achieved with MiniMACS (Miltenyi Biotec, Bergisch Gladbach, Germany). BCA Protein Assay Kit was from Pierce (Waltham, MA). Carboxyfluorescein diacetate succinimidyl ester (CFSE) was from Invitrogen (Camarillo, CA). Trypan blue, 7-amino-actinomycin D (7-AAD) were from Sigma. **Whole Cell Lysates:** Hep G2 whole cell lysate was purchased from Novus Biologicals (Littleton, CO) and employed for DLS, CD and mass spectrometry; A2780 ovary carcinoma lysate was gently provided by Prof. Banci's group (CERM, Florence, Italy) and employed for DLS, CD and mass spectrometry experiments, as well as for assays in the interaction between NPs@PC and DC; HCT-8 colon carcinoma lysate was obtained by HCT-8 colon carcinoma cell line kindly provided by Marcella Coronnello, (University of Florence).

Synthesis of NPs

Gold nanoparticles (AuNPs): AuNPs were synthesized following Turkevich et al. [21,22]. Briefly, 2 mL of 1% (wt/vol) trisodium citrate aqueous solution were rapidly injected into 20 mL of 1 mmol/L chloroauric acid ($HAuCl_4$) boiling solution under vigorous stirring. The formation of NPs was indicated by the colour change of the solution, which turns from the original pale yellow to burgundy. After 15 minutes the solution was cooled down in a water-ice bath. The AuNPs were

stored at 4°C and the dispersion was centrifuged (5 min -500 x *g*) at 15°C prior to use in order to remove aggregates.

Silica NPs (SiO_2NPs): SiO_2NPs were synthesized with the Stöber's process [23]. H_2O, EtOH and NH_4OH were mixed using a magnetic stirrer in a 40 ml Vial. TEOS was then added dropwise to the mixture while stirring. The solution was kept under stirring at room temperature for 48 hours.

Rhodamine B-labeled silica nanoparticles (RhB-SiO_2NPs): RhB-SiO_2NPs were prepared according to the work of Canton et al.[24] Briefly, they were prepared by hydrolysis and condensation of TEOS in ethanol in the presence of ammonia. To this aim, a solution containing appropriate quantities of absolute ethanol, ammonia and water was stirred for 5 minutes to ensure complete mixing. Rhodamine B isothiocyanate was added to the initial alkaline hydro-alcoholic solution to produce fluorescent NP; the mixture was left at room temperature overnight, under gentle stirring. Then a proper amount of TEOS in absolute ethanol was added and the reaction proceeded at room temperature for 48 h. The stable colloidal solution of NPs in water was separated from ammonia and ethanol by dialysis.

Coating of nanoparticles with a protein corona

The protocol adopted for the formation of the protein corona from lysates was the following: a determined amount of NPs (specified in the different sections) was incubated at room temperature with 200 µg/ml lysate under stirring. After 1 h, NPs were centrifuged at 8000 *g* for 10 min in order to separate them from unbound lysate. The procedure was repeated three times to ensure full removal of the unbound lysate. For DC maturation experiments, the protein content of the supernatant was quantified by BCA assay, in order to evaluate the amount of protein-bound lysate.

Cell Culture

Human buffy coats were obtained from healthy blood donors in the respect of Helsinki declaration and the Italian law and according to local ethic committee (authorization 0011762/2010). Monocyte-derived immature DC were obtained as previously reported [25]. NPs were added to DCs for 48 h while the concentration of FBS was reduced to 1% to minimize a possible influence of

serum factors on DCs maturation. In some experiments maturation-inducing cytokines [25] were added together with NPs. In control experiments, DCs were matured by cultivating them for 6 days in complete medium followed by 48 h with the further addition of maturation-inducing cytokinesì. Cells were checked by phase contrast microscopy throughout culture. Cell viability was assessed by Trypan blue absorption as well as by flow cytometry with 7-AAD staining

Allogeneic lymphocytes were recovered culturing PBMCs (isolated as above described from donors others than those from whom monocytes had been harvested) for 45 min in complete medium and harvesting suspended cells. The latter cells were centrifuged at 160 x *g*, for 10 min at 20°C, counted and used for mixed lymphocyte culture.

Interaction of NPs with DCs

Uncoated NPs were added to immature DCs at concentrations of 10 and 100 µg/mL, in order to assess uptake, intracellular distribution, cell viability and maturation. Nanoparticles functionalized with 10 µg/mL cell lysate were added at concentration of 25 and 75 µg/mL for SiO_2NPs and AuNPs respectively, in order to have the same coated surface area exposed per unit volume of culture medium. The conditions of challenge of DCs are specifically described in the SI.

RESULTS & DISCUSSION

Nanoparticles' characterization

SiO_2NPs and AuNPs were chosen as the prototypes of biocompatible inorganic NPs, of easy and tunable synthesis, that can be convenient carriers for applications in cancer immunotherapy. The simplest and most established synthesis protocols (Stöber[23] and Turkevich-Frens[21,22] for SiO_2NPs and AuNPs, respectively), described in details in the material and methods section, were adopted.

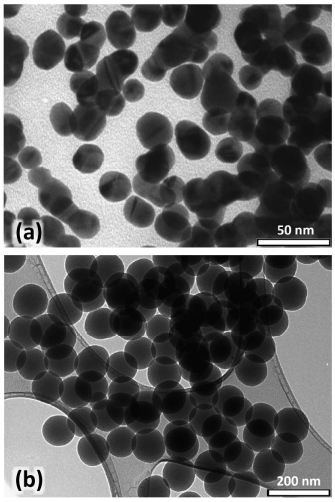

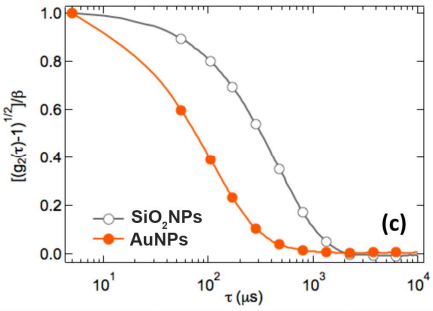

NPs	D_H [nm]	PDI	D [nm]	ζ-Pot. [mV]
SiO_2NPs	132 ± 5	0.01	104 ± 5	-53 ± 5
AuNPs	35 ± 2	0.15	20 ± 2	-26 ± 5

(d)

Figure 1. Characterization of NPs. (a, b) Representative TEM images of (a) gold NPs (AuNPs) and (b) silica NPs (SiO_2NPs); (c) Representative normalized autocorrelation functions of the scattered intensity of AuNPs (red line and filled markers) and SiO_2NPs (green line and empty markers), which give information on the hydrodynamic size of the NPs; (d) Summary of the main physicochemical features of the NPs: hydrodynamic diameter as obtained from DLS through cumulant fitting stopped at the second order (D_H) and related polydispersity index (PDI); diameter of the NPs (D) evaluated from TEM; zeta potential (ζ-Pot.) of the NPs.

Figure 1 reports the main physicochemical features of the NPs. Figure 1a and 1b display representative TEM images of AuNPs and of SiO_2NPs, respectively, which indicate the average diameter of the synthesized NPs as: 20 ± 2 nm for AuNPs and 104 ± 5 nm for SiO_2NPs (see Table in Figure 1d). Figure 1c displays representative normalized DLS curves of the same NPs. From the comparison of the profiles of the autocorrelation functions (ACF) of the scattered intensity it is clear that DLS is consistent with TEM. From the analysis of the ACFs through the cumulant fitting stopped at the second order it is possible to evaluate the hydrodynamic diameter (D_H) and the polydispersity index (PDI) of the two samples, reported in Figure 1d, whose values are slightly higher with respect to those obtained by TEM analysis. Both Turkevich-Frens and Stöber syntheses allow varying the synthetic procedure to tune the size of the obtained NPs. Finally, the table reported in Figure 1d contains the zeta potential values obtained for the aqueous dispersions of the two types of: both SiO_2NPs and AuNPs are characterized by a negative zeta potential, due to the presence of silanol groups on the surface of SiO_2NPs and the electrically stabilizing coating of

AuNPs by the citrate anion, respectively. The relatively high negative surface charge of the NPs might decrease the ability of the NPs to interact with the DC cell membrane (which is negatively charged as well) and to be internalized. However, in the design of nanostructured materials it is necessary to provide colloidal stability, while avoiding toxic effects (that are generally present when cationic NPs are employed). In summary, two types of NPs were synthesized through common, well-established synthetic procedures, leading to NPs with different core nature, size and zeta potential.

Interaction of nanoparticles with cancer cell lysates

Composition, size and charge of NPs are expected to have a major influence in the formation of NP-protein corona complexes. The Nanoparticles synthesized as described in the previous section were incubated with ovarian cancer cells lysate (A2780) or with hepatic cancer cells lysate (Hep G2), according to the protocol described in the experimental section, and then purified through repeated centrifugation to eliminate the unbound lysate. Finally, the coronated NPs (indicated as AuNPs@PC and SiO_2NPs@PC) were dispersed in ultrapure water and analyzed through DLS, zeta potential and CD to characterize the protein corona layer.

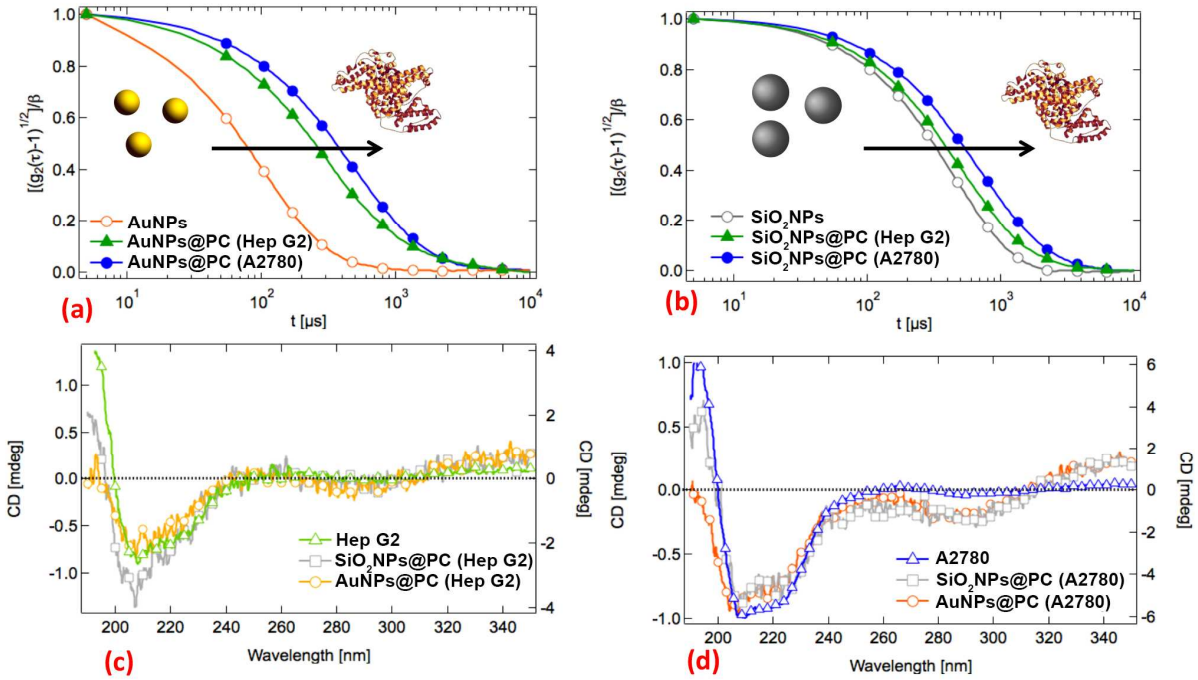

Figure 2. Protein corona formation. (a,b) Representative DLS curves acquired for (a) AuNPs and (b) SiO_2NPs in before (orange for AuNPs and grey for SiO_2NPs lines and empty circles) and incubated with Hep G2 (green lines and filled triangles) and A2780 (blue lines and filled circles) cell lysates; (c,d) CD spectra registered for (c) bare Hep G2 cell lysate (green line and empty triangles) and Hep G2 lysate-coated SiO_2NPs@PC (grey line and empty squares), AuNPs@PC (yellow line and empty circles); (d) bare A2780 lysate (blue line and empty triangles) and A2780 lysate-coated SiO_2NPs@PC (grey line and empty squares), AuNPs@PC (orange line and empty circles).

Figure 2a-b reports the representative DLS profiles of AuNPs (Figure 2a) and SiO_2NPs (Figure 2b) before and after formation of the protein corona from Hep G2 and A2780 lysates. For both kinds of NPs, incubation leads to a clear increase of the decay times of the ACF and to a change of curve slope, ascribable to the formation of larger and more polydisperse objects with respect to neat NPs, clearly due to the interaction with the biomolecules. Zeta potential measurements on the same samples confirm this hypothesis. Upon incubation with the cell lysate a value of -30 mV is obtained for both types of NPs, in spite of their different starting surface potential, diameter and coating, possibly indicating that a similar surface modification has occurred for both types of NPs. From the ACF profiles, displayed in Figure 2a-b, two interesting effects are clearly highlighted: first, both for SiO_2NPs and for AuNPs the decay of the ACF is longer for exposure of the NPs to A2780 than to Hep G2. Moreover, it can be observed that for both lysates the variation in the ACF profiles is much more marked for AuNPs than SiO_2NPs. Both effects clearly highlight that the formation of NP-protein corona assembly is not a random process and that the physicochemical characteristics of the NPs and the composition of the biological medium determine the final architecture. The analysis of the DLS curves through the cumulant fitting stopped at the second order provides the hydrodynamic diameter and polydispersity of NPs@PC, summarized in Table 1. Comparing the hydrodynamic diameters for the coronated nanoparticles (NPs@PC) with those obtained for the naked NPs, it is possible to estimate the thickness of the protein shell, also reported in Table 1. Consistently with the ACFs' profiles of the, the protein corona is thinner for Hep G2 (around 25 nm for SiO_2NPs and 52 nm for AuNPs coated by Hep G2

lysate vs. 62 nm and 109 nm for A2780 cell lysate-covered SiO_2NPs and AuNPs, respectively). Moreover, the corona is thicker for AuNPs than SiO_2NPs (see Table 1). These values are higher than what reported in the literature for typical protein corona thicknesses of SiO_2NPs and AuNPs in serum, [26,27]. This can be related to the different composition of whole cell lysates and serum, that probably determines a much more complex composition and structure of the corona decorating the surface of NPs, with a possibly multilayered architecture.

Lysate	D_H [nm]	PDI	PC [nm]
	SiO_2NPs@PC		
HepG2	182 ± 5	0.2	≈ 25
A2780	256 ± 9	0.2	≈ 62
	AuNPs@PC		
HepG2	140 ± 8	0.4	≈ 52
A2780	183± 9	0.2	≈ 109

Table 1. Protein corona DLS characterization. DLS data on the protein corona formed on SiO_2NPs (SiO_2NPs@PC) and AuNPs (AuNPs@PC) from Hep G2 and A2780 whole cell lysates, respectively; hydrodynamic diameter (D_H) and polydispersity index (PDI) of the protein-corona coated NPs, as obtained from the cumulant fitting stopped at the second order of the DLS experimental curves; estimated thickness of the protein corona (PC) calculated from the difference between the hydrodynamic diameter of NPs@PC and bare NPs, estimated from DLS, divided by two.

Figures 2c and 2d compare the CD spectra measured for cell lysates from A2780 (Figure 2c) and Hep G2 (Figure 2d) with those obtained for the AuNPs@PC and SiO_2NPs@PC after exposure to the two lysates. The spectra recorded for AuNPs@PC and SiO_2NPs@PC, show a clear CD effect in the wavelength range between 230 and 190 nm, typically referred to proteins, further confirming the formation of the protein corona for both NPs in both cell lysates. From the comparison of the spectra obtained with the two lysates, we can notice that the minimum at 210 nm, present in both samples, is more pronounced in the ovarian cancer lysate (Figure 2d), possibly indicating a compositional difference of the two lysates that can be consistent with the previously discussed differences in the protein corona formation. However, the lysates contain many different biomolecules and proteins and the attribution of the CD profile to a single class of componenets is

not possible. While some qualitative conclusions can be drawn, with this method it is not possible to determine any compositional differences in the protein corona of SiO_2NPs@PC and AuNPs@PC.

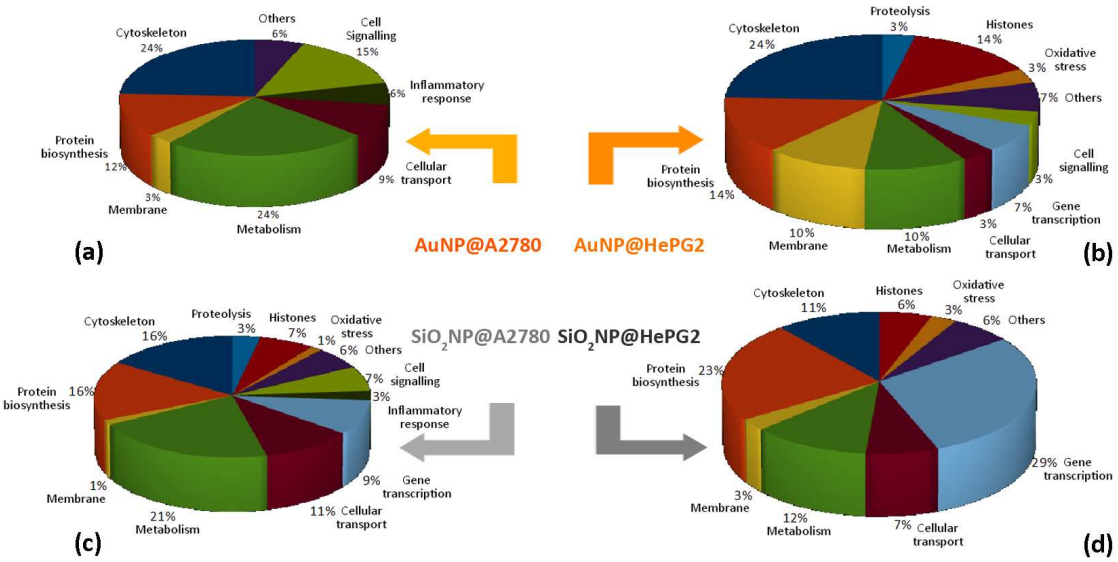

Figure 3. Composition of SiO_2NP@PC and AuNP@PC Composition of the protein corona of (a, b) AuNPs@PC and (c,d) SiO_2NP@PC upon incubation with (a,c) A2780 cell lysate and (b,d) Hep G2 cell lysate. The differences in composition between the coronas of Au and SiO_2 NPs with A2780 and Hep G2 lysates are summarized in these four charts. For each combination of nanoparticle type and lysate are reported the proteins contained classified by their biological function. Au and SiO_2 NPs clearly bind different libraries of proteins. This is true considering the protein corona obtained from the same lysate on the two different nanoparticles, but also comparing the pool of proteins adsorbed on the same nanoparticle from the two different lysate.

In order to identify the protein corona composition, the protein shells of the NPs, were analyzed by mass spectrometry. The shotgun mass spectrometric approach allowed the identification of 499 proteins (Table S4, supporting information) for the ovarian cancer lysate and 84 proteins for the Hep G2 lysate (Table S1, supporting information). The marked difference between the number of proteins identified for A2780 and Hep G2 can be tentatively explained by assuming a non-complete removal of the protease inhibitor cocktail originally present in the Hep G2 sample (Hep G2 is a commercial lysate, unlike A2780 lysate), which partially inhibits protein digestion. Concerning the composition of the protein corona, the main results are summarized in Figure 3 for both nanoparticles. As highlighted in the mass spectrometry data extensively reported in the SI, a first

difference is represented by the number of proteins bound on AuNPs and SiO_2NPs from both A2780 and Hep G2 lysates. In the coronas adsorbed from hepatic cancer lysate 109 proteins were identified for SiO_2NPs and 30 proteins for AuNPs. Similarly, from ovarian cancer lysate, 75 proteins were adsorbed on SiO_2NPs and 33 proteins on AuNPs. Thus, Silica NPs bind a double (for A2780) and triple (for Hep G2) amount of proteins. According to literature, gold has a preferential affinity for some amino acidic residues [28]. Therefore, the higher number of different proteins adsorbed on SiO_2NPs can be due to a lower specificity.

The proteins list was then analyzed using three different protein databases: The Human Protein Atlas, UniProtKB and the National Center for Biotechnology Information (NCBI). By crossing the information obtained from these databases, the proteins were classified according to their biological function. Comparing the coronas adsorbed from a single lysate, it is clear that AuNPs and SiO_2NPs bind different libraries of proteins, as shown in Figure 3. Considering Hep G2 lysate's coronas, it can be noticed that, while on AuNPs the highest percentage of protein is cytoskeleton-related, on SiO_2NPs, the highest percentage is related to gene transcription and protein biosynthesis. Moreover, on AuNPs, cell signaling and proteolytic proteins were identified, that are absent on SiO_2NPs. In the case of A2780 lysate the situation is different. SiO_2NPs are able to bind histones and oxidative stress, proteolytic and gene transcriptional proteins, that were not found on AuNPs. The highest percentages of proteins, though, are represented by metabolism and cytoskeleton related ones for both NPs.

Summarizing these observations, we can state that AuNPs and SiO_2NPs are not only able to bind different libraries of protein from one kind of lysate, but they can also select different classes depending on the lysate source. Using The Human Protein Atlas, we extended further this analysis. In the coronas adsorbed from both lysates, some cancer related proteins were identified. In particular, for A2780 on SiO_2NPs, 15 cancer related proteins are present, 12 of which are scarce or absent in healthy tissues, while on AuNPs 11 cancer related proteins are found, scarcely present or absent in healthy subjects. For SiO_2NPs-Hep G2 lysate corona 23 proteins are cancer related, 8 of

which scarce or absent in healthy subjects, while on AuNPs the cancer related proteins are 7, including Tubulin α1A chain, scarce in healthy tissues. Moreover, using the same database, we verified that the NPs are coated with six proteins been recognized as FDA-approved drug targets for cancer. Four of them are bound to SiO_2NPs, and the remaining two to AuNPs.

In summary, these results confirm the selective nature of protein adsorption on NPs from biological media, depending on the chemical nature of the particle core. Moreover, this protein corona is enriched in some classes of proteins, if compared to its cell lysate source. The ability to concentrate disease-related biomolecules is particularly important in view of the therapeutic applications of these NPs. For the purposes of this study, the NPs were tested concerning their ability to stimulate dendritic cells to trigger immunoresponse to cancer.

Interaction of nanoparticles with dendritic cells

In order to qualitatively monitor the interaction and internalization of the NPs, in the absence and in the presence of their protein coating, with DCs cells, we performed a TEM and fluorescence microscopy investigation. In particular, while electron microscopy is especially suitable to monitor the highly electrondense AuNPs, the exact SiO_2NPs intracellular localization by means of TEM is more elusive, due to the lower contrast. To this aim, Rhodamine-labeled SiO_2NPs (RhB-SiO_2NPs) were synthesized, [24] as described in the experimental section, and characterized (SI, Figure S1), to be monitored with fluorescence microscopy.

Figure 4 summarizes the microscopy data collected for the different NPs and NPs@PC. Fluorescence microscopy showed that the interaction between RhB-SiO_2NPs and DCs is fast and leads to NPs' internalization (Fig 4a-d). Quantitative analysis of fluorescence (see SI, Figure S2) showed that both the number of cells internalizing NPs and the fluorescence intensity per cell, connected to the amount of NPs internalized, depend on NPs' concentration. Both values were significantly higher with 100 μg/mL than 10 μg/mL NPs; they did not increase significantly between 4 and 24 h incubation for both concentrations of NPs, indicating that the maximum load

per responsive cell was reached in a short time. A possible explanation is that the particles are recycled from lysosomes outside the cell by exocytosis, so that the amount present in a cell at any moment after a steady state is reached depends on the concentration of NPs in the medium. The results were independent of the addition of maturation-stimulating cytokines.

Concerning AuNPs, TEM showed that AuNPs were uptaken through endocytosis and then localized in endosomes and lysosomes, similarly to what reported in the literature [29,30], as displayed in Figure 4e-g.

The negative surface charge of NPs is expected to induce electrostatic repulsion with negatively charged cellular membrane, limiting their ability to interact with cells. Our results show that both type of NPs are effectively internalized by DCs, confirming the small effect of negative charge on internalization by phagocytic cells [29]. Moreover, no significant differences in internalization were detected in the absence and in the presence of protein corona, for both SiO_2NPs and AuNPs. The efficient internalization of corona-coated NPs is particularly interesting and unexpected: generally, it is well-established that the passivation of NPs with the protein corona shell decreases the surface energy of NPs and, thus, the tendency of NPs to interact with biomembranes and to be internalized by cells [31,32]. In the present case, the NP@PC complexes, coated with cancer cell lysates, efficiently interact and are internalized by DCs, with no appreciable difference with respect to the as-synthesized ones,

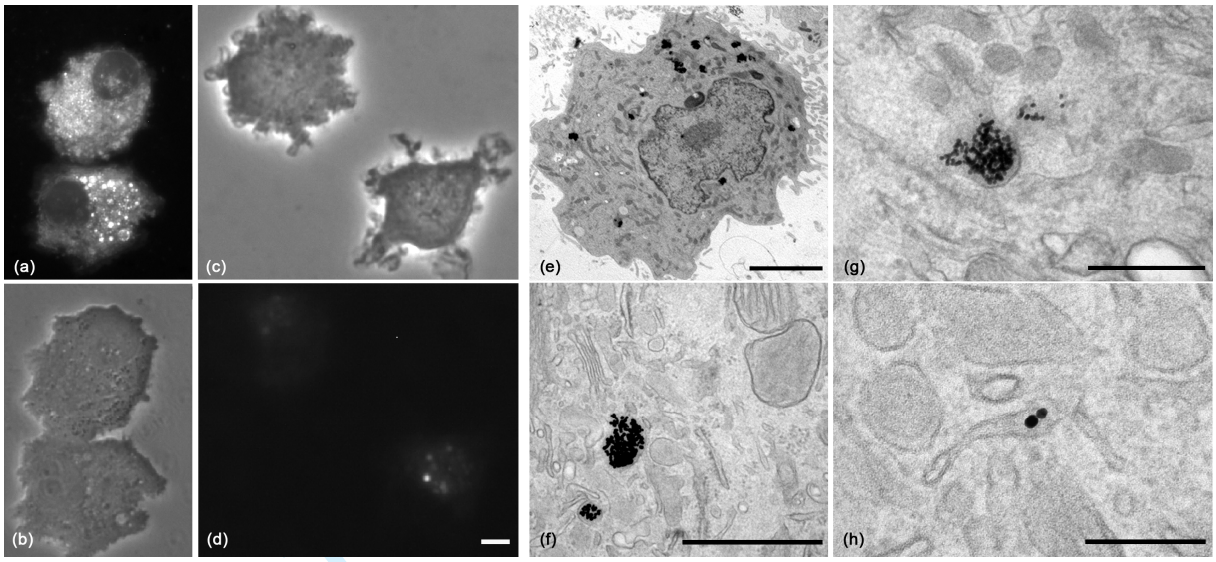

Figure 4. Interaction of NPs and NPs@PC with DCs: internalization Fluorescence microscopy images of (a,b) RhB-SiO_2NPs and (c,d) RhB-SiO_2NPs@PC uptake by DCs after 24 hours from addition; bar = 10 µm; (e-h) TEM of DCs incubated 48 h with (e, f) AuNPs and (g,h) Au-NPs@PC; bars = 2µm (e), 1 µm (f), 500 nm (g), 100 nm (h). NPs appeared in small vesicles and in larger vacuoles mainly in the Golgi area, representing late endosomes and lysosomes

Besides internalization, the same NPs in the absence and in the presence of protein corona coating were also tested in terms of biocompatibility. Challenge with both types of NPs, did not lead to the appearance of signs of cell sufferance or death, as judged by light and electron microscopy and exclusion of trypan blue.[30]. Flow cytometry also confirmed that NPs were not cytotoxic (Supplementary Table S7), in line with what reported in the literature. [33-35] Our data agree with the results of Tomic et al. showing that different sized Au-NPs from 10 to 50 nm are not toxic between 10 and 200 µg/ml. Kunzmann [33] reported that silica coated iron oxide NPs were non-toxic for human monocyte derived cells, at all concentration tested, while they found a dose-dependent toxicity for primary Mo-DCs with smaller silica-coated nanoparticles (30 nm and 50 nm). A size-dependent and cellular type-dependent effect has been also reported, indicating a higher toxicity on macrophages with respect to endothelial cells [34]. Nabeshi has demonstrated that the cellular uptake and cytotoxicity increased with reduction in particle size [35], using mouse

epidermal Langerhans cell line XS52 treated with silica particles with diameter of 70, 300, or 1000 nm.

Both SiO_2NPs and AuNPs are thus efficiently endocyted and non toxic and could therefore be a particularly attractive carrier for clinical applications [36].

In Figure 5 the maturation profile of the DCs challenged with the NPs at two different concentrations (10 µg/ml and 100 µg/ml) is compared to that of immature DCs (Imm, negative control) and to DCs stimulated with inflammatory cytokines (positive control). The maturation profile of DCs showed that NPs did not significantly influence immature DCs phenotype, as demonstrated by maturation markers expression, with the exception of CD86 following 100 µg/ml AuNPs, which was significantly upregulated (23 ± 8% and 66 ± 8% for DCs without NPs and DCs with 100 µg/ml AuNPs, respectively). However, DCs were not fully matured as demonstrated by lymphocyte proliferation (see Figure 6b). This is in line with Vallhov, who reported that human monocyte-derived DCs (Mo-DCs), did not fully maturated when co-cultured with NPs, even if there was a significant increase of CD86 positive cells [37]. Thus, we can conclude that, even if some effects on CD86 marker are observed upon exposition of DCs to NPs, this is not related to DC maturation, and the effect of both types of NPs on the maturation of the DCs has to be considered negligible.

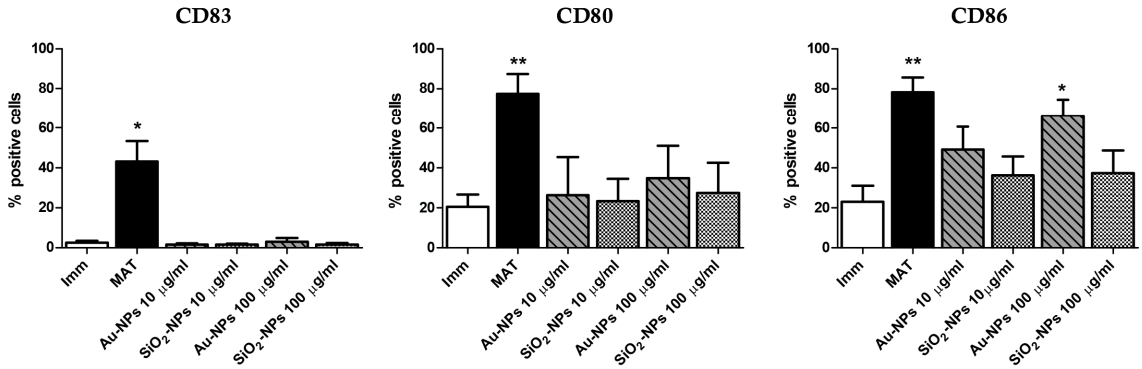

Figure 5. Interaction of NPs with DC: maturation DC maturation with nude SiO_2NPs and AuNPs, 10 e 100 µg/ml. Imm = immature DCs; MAT = DCs stimulated with inflammatory cytokines (positive control); SiO_2NPs or AuNPs 10 µg/ml and SiO_2NPs or AuNPs 100 µg/ml =

DCs incubated with SiO_2NPs or AuNPs at 10 and 100 µg/ml, respectively. Mean ± SE, N=6; *P<0,05 and **P<0,01 vs Imm.

Finally, we tested the interactions of the coronated NPs with DCs, to verify their immunogenic potential. In order to correctly compare AuNPs@PC and SiO_2NPs@PC, different NPs' amounts were chosen (75 µg/ml and 25 µg/ml for AuNPs and SiO_2NPs, respectively, both within the range of ineffectiveness on DCs), allowing the same exposed surface area toward cell lysate, evaluated taking into account the different sizes and densities of the cores, and co-cultured with immature DCs. In Figure 6a the maturation profile of the DCs challenged with the NPs@PC is displayed and compared to those of DCs challenged with the bare lysate and bare NPs, with immature DCs (negative control) and DCs stimulated with inflammatory cytokines (positive control). Clearly, the lysate alone provokes a significant increase in DC maturation, with respect to the immature DCs, which is not increased in the presence of NPs. Nevertheless, a clear difference is observed in the effects of AuNPs and SiO_2NPs on DC maturation. The incubation of immature DCs with NPs@PC showed that the presence of a protein corona triggered a significant increase in the expression of CD80 and CD83 when cells where incubated with protein coated AuNPs@PC, as compared with immature DCs. The increase, expressed as percentage values of immature DC, was 21.3 ± 5.5% for CD80 and 15.2 ± 4.4% for CD83. Such an increase was not observed with SiO_2NPs@PC. Thus, notwithstanding the same amount of lysate transported by the two NPs to the DCs, a different biological response is observed for the SiO_2NPs and AuNPs, that can be attributed either to the sole different composition, size and charge of the NPs, or to the different pool of adsorbed proteins in the corona.

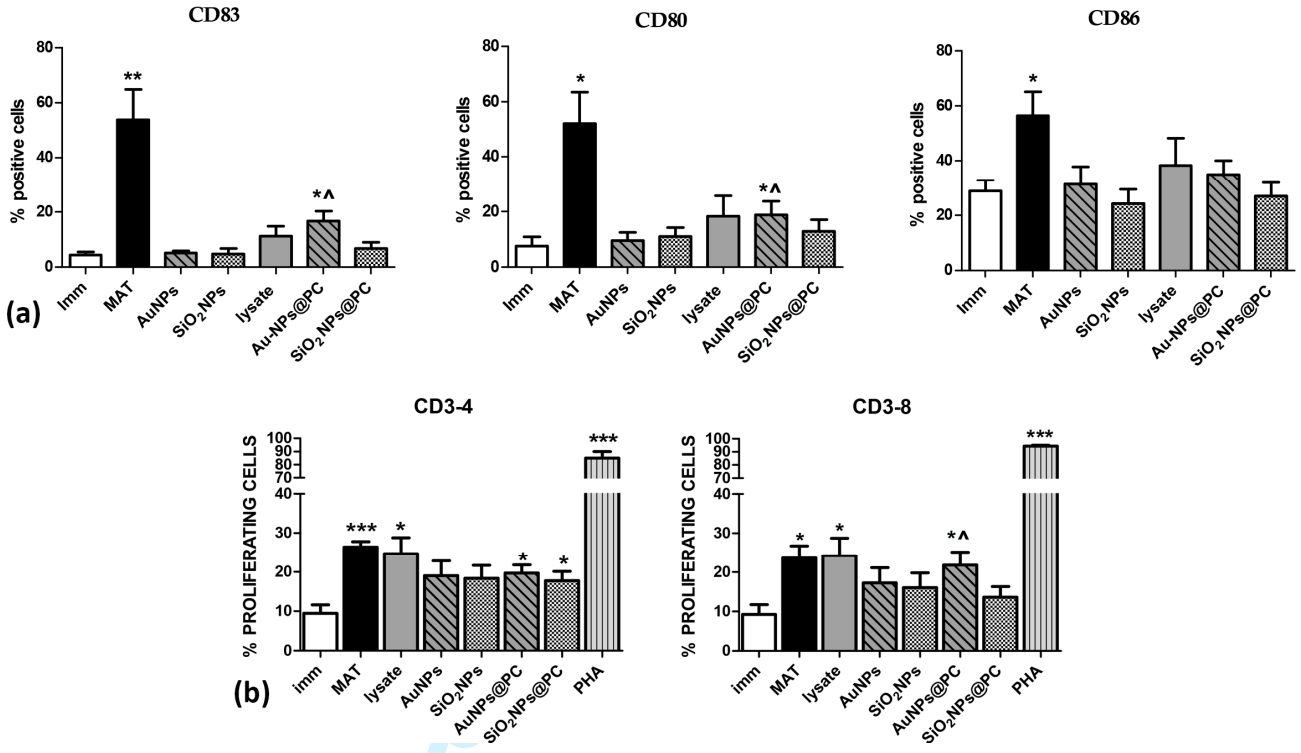

Figure 6. a Interaction of NPs@PC with DC: a) DC maturation with lysate-functionalized NPs. Imm = immature DCs; MAT= DCs stimulated with inflammatory cytokines (positive control); AuNPs = immature DCs incubated with 75 µg/ml AuNPs; SiO_2NPs = immature DCs incubated with 25 µg/ml SiO_2NPs; lysate = immature DCs incubated with 10 µg/ml lysate (without NPs); AuNPs@PC = DCs incubated with AuNPs (75 µg/ml) coated with 10 µg/ml lysate; SiO_2NPs@PC = DCs incubated with SiO_2NPs (25 µg/ml) coated with 10 µg/ml lysate. Mean ± SE; N = 4; *P<0,05 e **P<0,01 vs Imm; ^P<0.05 vs SiO_2NP + lys ADS. **b** Mixed lymphocyte reaction. T lymphocyte proliferation in response to DC treated with NPs and 10 µg/ml of tumor lysate, as measured by CFSE dilution assay. Imm = lymphocytes incubated with immature DCs; MAT = lymphocytes incubated with DCs matured with inflammatory cytokines (positive control); lysate = lymphocytes incubated with DCs pulsed with 10 µg/ml lysate; AuNPs = lymphocytes incubated with DCs pulsed with 75 µg/ml of AuNPs; SiO_2NPs = lymphocytes incubated with DCs pulsed with 25 µg/ml of SiO_2NPs; AuNPs@PC = lymphocytes incubated with DCs pulsed with 75 µg/ml of Au-NPs adsorbed with 10 µg/ml of tumor lysate; SiO_2NPs@PC = lymphocytes incubated with DCs pulsed with 25 µg/ml of SiO_2NPs adsorbed with 10 µg/ml of tumor lysate; PHA = lymphocytes stimulated with [5 µg/ml] phytohaemoagglutinin (without DCs). Mean ± SE; N = 4; *P<0,05, ***P<0,001 vs Imm; ^P<0.05 vs SiO_2NPs@PC.

As a final experiment, we assessed the effect of NPs@PC on DC ability to stimulate lymphocyte proliferation. The main results are displayed in Figure 6b. DC-treated with uncoated SiO_2NPs or AuNPs did not stimulate lymphocyte proliferation significantly. The proliferative response of both $CD4^+$ and $CD8^+$ lymphocytes to DCs treated with proteins of cell lysate - without NPs - was

significantly higher than that elicited by immature DCs and comparable to that elicited by mature DCs -without lysate nor NPs -. The proliferation induced by DCs treated with NPs@PC never exceeded that achieved with DCs treated with lysate alone. Even if it has been reported that proteins coated on NPs may undergo conformational changes, leading to the exposure of new epitopes [38], many studies reported that only a few tumor associated antigens (about 10%) exert immunogenicity and among them only very few are effectively associated with tumor rejection [39]. However, consistently with what observed in the previously discussed experiment on DC maturation (Figure 6a), a clear difference is observed in the effects of AuNPs@PC and SiO_2NPs@PC: DCs treated with AuNPs@PC were able to induce both $CD4^+$ and $CD8^+$ proliferation, while SiO_2NPs@PC-treated DCs stimulated significantly the proliferation only of $CD4^+$ lymphocytes ($P<0.05$, $n=5$). The increase of $CD4^+$, however, could be also due to Treg expansion, considering the low maturation profile of DCs treated with lysate alone or SiNPs@PC. A clear difference between the biological response of DCs to the two types of NPs is thus observed.

CONCLUSION

In this work we exploited the spontaneous tendency of inorganic NPs in biological media to decorate their surface with a protein corona coating, to build-up a self-assembled nanocarrier for possible application in cancer immunotherapy. Two simple nanoparticles, Turkevich-Frens citrated AuNPs and Stober SiO_2NPs were chosen as prototypes of easy-synthesized biocompatible NPs of different composition, size and charge. We demonstrated that both NPs, exposed to cancer cells lysates decorate their surface with a protein corona coating, of different composition depending on the lysate biological origin and the physicochemical features of the NPs. When incubated with immature DCs, no toxicity effects were detected, while both NPs, in the absence and in the presence of the protein corona coating, where efficiently internalized. Finally, significant differences were observed in the biological response of immature DC to SiO_2NPs@PC and AuNPs@PC and in the

induced Lymphocytes T proliferation, suggesting that the different composition and physicochemical features of the NPs, determining a different composition of their protein corona coating from cells' lysates, can in turn determine a different biological response of the DCs to the system. This is indeed a promising result, representing a first step to exploit the spontaneous self-assembly of the protein corona on NPs' surface to build-up a simple, cost-effective, easy synthesized and tunable inorganic NPs-based nanocarrier for cancer vaccines application.

REFERENCES

[1] Fan Y, Moon JJ. Nanoparticle drug delivery systems designed to improve cancer vaccines and immunotherapy. *Vaccines* 3 (3), 662-685 (2015).

[2] Banchereau J, Steinman RM. Dendritic cells and the control of immunity. *Nature* 392, 245–252 (1998).

[3] Rosenberg SA, Yang JC, and Restifo NP. Cancer immunotherapy: moving beyond current vaccines. *Nature medicine* 10 (9), 909–15 (2004).

[4] June CH. Principles of adoptive T cell therapy for cancer therapy. *The Journal of Clinical Investigation* 117, 1204–1212 (2007).

[5] Banchereau J, Steinman RM. Dendritic cells and the control of immunity. *Nature* 392, 245–252 (1998).

[6] Palucka K and Banchereau J. Dendritic-cell-based therapeutic cancer vaccines. *Immunity* 39 (1), 38–48 (2013).

[7] Silva JM, Vandermeulen G, Oliveira VG, Pinto SN, Rodrigues C, Salgado A, Afonso CA, Viana AS, Jerôme C, Silva LC, Graca L, Préat V, Florindo HF. Development of functionalized nanoparticles for vaccine delivery to dendritic cells: a mechanistic approach. *Nanomedicine* 9 (17), 2639-2656 (2014).

[8] Foerster F, Bamberger D, Schupp J, Weilbächer M, Kaps L, Strobl S, Radi L, Diken M, Strand D, Tuettenberg A, Wich PR, Schuppan D. Dextran-based therapeutic nanoparticles for hepatic drug delivery. *Nanomedicine* 11(20), 2663-2677, (2016).

[9] Shen L, Krauthäuser S, Fischer K, Hobernik D, Abassi Y, Dzionek A, Nikolaev A, Voltz N, Diken M, Krummen M, Montermann E, Tubbe I, Lorenz S, StrandD, Schild H, Grabbe S, Bros M. Vaccination with trifunctional nanoparticles that address CD8+ dendritic cells inhibits growth of established melanoma. *Nanomedicine* 11(20), 2647-2662 (2016)

[10] Tonigold M, Mailänder V. Endocytosis and intracellular processing of nanoparticles in dendritic cells: routes to effective immunonanomedicines. *Nanomedicine* 11(20), 2625-2630 (2016).

[11] Carter T, Mulholland P, Chester K. Antibody-targeted nanoparticles for cancer treatment. *Immunotherapy* 8(8), 941-958 (2016).

[12] Manuelli M, Fallarini S, Lombardi G, Sangregorio C, Nativi C, Richichi B. Iron oxide superparamagnetic nanoparticles conjugated with a conformationally blocked α-Tn antigen mimetic for macrophage activation. *Nanoscale* 6, 7643-7655 (2014).

[13] Parry AL, Clemson NA, Ellis J, Bernhard SR, Davis BG, Cameron NR. 'Multicopy Multivalent' Glycopolymer-Stabilized Gold Nanoparticles as Potential Synthetic Cancer Vaccines. *Journal of the American Chemical Society* 135, 9362-9365 (2013).

[14] Walkey CD and Chan WCW. Understanding and controlling the interaction of nanomaterials with proteins in a physiological environment. *Chemical Society Reviews* 41 (7), 2780–2799 (2012).

[15] Lundqvist M, Stigler J, Cedervall T, Berggård T, Flanagan MB, Lynch I, Elia G, Dawson KA. The evolution of the protein corona around nanoparticles: a test study. *ACS Nano* 5 (9), 7503–7509 (2011).

[16] Cedervall T, Lynch I, Lindman S, Berggård T, Thulin E, Nilsson H, Dawson KA, Linse S. Understanding the nanoparticle protein corona using methods to quantify exchange rates and affinities of proteins for nanoparticles. *Proceeding of the National Academy of Sciences* 104 (7), 2050–2055 (2007).

[17] Montis C, Maiolo D, Alessandri I, Bergese P, Berti D. *Nanoscale* 6, 6452 (2014)

[18] Walkey CD, Olsen JB, Guo H, Emili A, Chan WCW. *Journal of the American Chemical Society* 134, 2139-47 (2012).

[19] Walczyk D, Baldelli Bombelli F, Monopoli MP, Lynch I, Dawson KA. What the cell "sees" in bionanoscience. *Journal of the American Chemical Society* 132 (16), 5761–5768 (2010).

[20] Walkey CD, Olsen J.B., Song F, Liu R, Guo H, Olsen DWH, Cohen Y, Emili A, and Chan WCW. Protein Corona Fingerprint Predicts the Cellular Interaction of Gold and Silver Nanoparticles. *ACS Nano* 8 (3), 2439–2455 (2014).

[21] Turkevich J, Stevenson PC, Hillier J. J. Discussion Faraday Soc. 11,55 (1951).

[22] G Frens. Nature Physical Science. 20, 241 (1973).

[23] W Stöber, A Fink. Journal of colloid and interface science. 26, 62-69 (1968).

[24] Canton G, Riccò R, Marinello S, Carmignato F, and Enrichi F. Modified Stöber synthesis of highly luminescent dye-doped silica nanoparticles. *Journal of Nanopart. Res.* 13, 4349–4356, (2011).

[25] Paccosi S, Musilli C, Caporale R, Gelli AMG, Guasti D, Clemente AM, Torcia MG, Filippelli A, Romagnoli P, Parenti A. Stimulatory interactions between human coronary smooth muscle cells and dendritic cells. *PLOS One* 9 (6), e99652 (2014).

[26] Monopoli MP, Walczyk D, Campbell A, Elia G, Lynch I, Baldelli Bombelli F, Dawson KA. Physical-Chemical Aspects of Protein Corona: Relevance to in Vitro and in Vivo Biological Impacts of Nanoparticles. *Journal of the American Chemical Society* 133 (8), 2525–2534 (2011).

[27] Casals E, Pfeller T, Duschl A, Oostingh GJ, Puntes V. Time evolution of the nanoparticle protein corona. *ACS Nano* 4(7), 3623–3632 (2010).

[28] De Paoli-Lacerda SH, Park JJ, Meuse C, Pristinski D, Becker ML, Karim A, Douglas JF. Interaction of gold nanoparticles with common human blood proteins. *ACS Nano* 4, 365-379 (2010).

[29] Liu X, Huang N, Li H, Jin Q, Ji J, Surface and size effects on cell interaction of gold nanoparticles with both phagocytic and non-phagocytic cells. *Langmuir* 29(29), 9138-9148 (2013).

[30] Tomić S, Đokić J, Vasilijić S, Ogrinc N, Rudolf R, Pelicon P, Vučević D, Milosavljević P, Janković S, Anžel I, Rajković J, Rupnik MS, Friedrich B, Colić M. Size-dependent effects of gold nanoparticles uptake on maturation and antitumor functions of human dendritic cells in vitro. *PLoS One* 9(5), e96584 (2014).

[31] Maiolo D, Del Pino P, Metrangolo P, Parak WJ, Baldelli-Bombelli F. Nanomedicine delivery: does protein corona route to the target or off road? *Nanomedicine* 10 (21), 3231-3247 (2015).

[32] Lesniak A, Fenaroli F, Monopoli MP, Åberg C, Dawson KA, Salvati A. Effects of the presence or absence of a protein corona on silica nanoparticle uptake and impact on cells. *ACS Nano* 6 (7), 5845-5857 (2012).

[33] Kunzmann A, Andersson B, Vogt C, Feliu N, Ye F, Gabrielsson S, Toprak MS, Buerki-Thurnherr T, Laurent S, Vahter M, Krug H, Muhammed M, Scheynius A, Fadeel B. Efficient internalization of silica-coated iron oxide nanoparticles of different sizes by primary human macrophages and dendritic cells. *Toxicol Appl Pharmacol* 253(2), 81-93 (2011).

[34] Thomassen LC, Aerts A, Rabolli V, Lison D, Gonzalez L, Kirsch-Volders M, Napierska D, Hoet PH, Kirschhock CE, Martens JA. Synthesis and characterization of stable monodisperse silica nanoparticle sols for in vitro cytotoxicity testing. *Langmuir* 2 (1), 328-335 (2010).

[35] Nabeshi H, Yoshikawa T, Matsuyama K, Nakazato Y, Arimori A, Isobe M, Tochigi S, Kondoh S, Hirai T, Akase T, Yamashita T, Yamashita K, Yoshida T, Nagano K, Abe Y, Yoshioka Y, Kamada H, Imazawa T, Itoh N, Tsunoda S, Tsutsumi Y. Size-dependent cytotoxic effects of amorphous silica nanoparticles on Langerhans cells. *Pharmazie* 65 (3), 199-201 (2010).

[36] Park YM, Lee SJ, Kim YS, Lee MH, Cha GS, Jung ID, Kang TH, Han HD. Nanoparticle-based vaccine delivery for cancer immunotherapy. *Immune Netw* 13 (5), 177-183 (2013).

[37] Vallhov H, Gabrielsson S, Strømme M, Scheynius A, Garcia-Bennett AE. Mesoporous silica particles induce size dependent effects on human dendritic cells. *Nano Lett* 7 (12), 3576-3582 (2007).

[38] Lundqvist M, Stigler J, Elia G, Lynch I, Cedervall T, Dawson KA. Nanoparticle size and surface properties determine the protein corona with possible implications for biological impacts. *Proc Natl Acad Sci* USA 105 (38), 14265-70 (2008).

[39] Kroemer G, Zitvogel L. Can the exome and the immunome converge on the design of efficient cancer vaccines? *Oncoimmunology* 1 (5), 579-580 (2012).

SUPPLEMENTARY DATA

Supplementary data and methods, including the complete mass spectrometry results, the full physicochemical RhB-SiO_2NPs characterization and the quantitative fluorescence microscopy analysis on RhB-SiO_2NPs interacting with DCs are available at the journal website.

FINANCIAL AND COMPETING INTEREST DISCLOSURE

The authors declare no competing interests.

SUMMARY POINTS

- The spontaneous formation of nanoparticles-protein complexes, obtained from interaction of NPs with cancer cells lysates is investigated, to build-up nanodevices for potential application in cancer immunotherapy.
- Gold and Silica NPs were synthesized through simple synthetic routes and exposed to different cancer cells' lysates: this leads to the spontaneous association of NP complexes with biomolecules, in particular cancer-related proteins and FDA-approved cancer therapy targets.
- Gold and Silica NPs exhibit a different behavior when exposed to the same lysates: they bind different pools of proteins and exhibit a different specificity towards the same protein classes. The NP's nature determines the physicochemical features and composition of the final nanodevice.
- Gold and Silica NPs, in the absence and in the presence of the protein corona coating, are non toxic and efficiently internalized by dendritic cells.
- No effects on the maturation of dendritic cells is induced by the bare nanoparticles in the absence of protein corona coating, while nanoparticles-protein corona complexes, affect the maturation of dendritic cells.
- A clear difference between the behavior of gold nanoparticles-protein corona and of silica nanoparticles-protein corona complexes is observed both in promoting the maturation of dendritic cells and T lymphocyte proliferation.
- In summary, the different physicochemical features of the core of the nanoparticles (composition, size, surface charge) determine the composition of the protein corona and the interaction with dendritic cells.

Supporting Information for:

Inorganic Nanoparticles as Potential Regulators of Immune Response in Dendritic Cells

Supplementary Figures and Tables

	Hep G2 cell lysate
1	60 kDa heat shock protein, mitochondrial OS=Homo sapiens GN=HSPD1 PE=1 SV=2
2	Actin, cytoplasmic 1 OS=Homo sapiens GN=ACTB PE=1 SV=1
3	Histone H2B type 1-M OS=Homo sapiens GN=HIST1H2BM PE=1 SV=3
4	Ribosome-binding protein 1 OS=Homo sapiens GN=RRBP1 PE=1 SV=4
5	10 kDa heat shock protein, mitochondrial OS=Homo sapiens GN=HSPE1 PE=1 SV=2
6	Keratin, type II cytoskeletal 1 OS=Homo sapiens GN=KRT1 PE=1 SV=6
7	Prelamin-A/C OS=Homo sapiens GN=LMNA PE=1 SV=1
8	Serum albumin OS=Homo sapiens GN=ALB PE=1 SV=2
9	Heterogeneous nuclear ribonucleoprotein A1 OS=Homo sapiens GN=HNRNPA1 PE=1 SV=5
10	Histone H3.1t OS=Homo sapiens GN=HIST3H3 PE=1 SV=3
11	Keratin, type I cytoskeletal 19 OS=Homo sapiens GN=KRT19 PE=1 SV=4
12	Triosephosphate isomerase OS=Homo sapiens GN=TPI1 PE=1 SV=3
13	Keratin, type I cytoskeletal 9 OS=Homo sapiens GN=KRT9 PE=1 SV=3
14	Metallothionein-1E OS=Homo sapiens GN=MT1E PE=1 SV=1
15	Heterogeneous nuclear ribonucleoprotein M OS=Homo sapiens GN=HNRNPM PE=1 SV=3
16	Heat shock protein HSP 90-beta OS=Homo sapiens GN=HSP90AB1 PE=1 SV=4
17	Tubulin alpha-1A chain OS=Homo sapiens GN=TUBA1A PE=1 SV=1
18	78 kDa glucose-regulated protein OS=Homo sapiens GN=HSPA5 PE=1 SV=2
19	Histone H2A type 1-C OS=Homo sapiens GN=HIST1H2AC PE=1 SV=3
20	Nucleolin OS=Homo sapiens GN=NCL PE=1 SV=3
21	Thioredoxin domain-containing protein 5 OS=Homo sapiens GN=TXNDC5 PE=1 SV=2
22	L-lactate dehydrogenase A chain OS=Homo sapiens GN=LDHA PE=1 SV=2
23	Protein disulfide-isomerase OS=Homo sapiens GN=P4HB PE=1 SV=3
24	U3 small nucleolar RNA-interacting protein 2 OS=Homo sapiens GN=RRP9 PE=1 SV=1
25	Fructose-bisphosphate aldolase A OS=Homo sapiens GN=ALDOA PE=1 SV=2
26	Malate dehydrogenase, mitochondrial OS=Homo sapiens GN=MDH2 PE=1 SV=3
27	Isocitrate dehydrogenase [NADP] cytoplasmic OS=Homo sapiens GN=IDH1 PE=1 SV=2
28	Elongation factor 1-alpha 1 OS=Homo sapiens GN=EEF1A1 PE=1 SV=1
29	Single-stranded DNA-binding protein, mitochondrial OS=Homo sapiens GN=SSBP1 PE=1 SV=1
30	Proteasome subunit alpha type-6 OS=Homo sapiens GN=PSMA6 PE=1 SV=1
31	Sodium/potassium-transporting ATPase subunit alpha-1 OS=Homo sapiens GN=ATP1A1 PE=1 SV=1
32	Solute carrier family 2, facilitated glucose transporter member 1 OS=Homo sapiens GN=SLC2A1 PE=1 SV=2
33	Transferrin receptor protein 1 OS=Homo sapiens GN=TFRC PE=1 SV=2
34	DNA replication licensing factor MCM5 OS=Homo sapiens GN=MCM5 PE=1 SV=5
35	60S ribosomal protein L28 OS=Homo sapiens GN=RPL28 PE=1 SV=3
36	Dolichyl-diphosphooligosaccharide--protein glycosyltransferase subunit STT3A OS=Homo sapiens GN=STT3A PE=1 SV=2
37	Apolipoprotein E OS=Homo sapiens GN=APOE PE=1 SV=1
38	UDP-glucose 6-dehydrogenase OS=Homo sapiens GN=UGDH PE=1 SV=1
39	Delta(3,5)-Delta(2,4)-dienoyl-CoA isomerase, mitochondrial OS=Homo sapiens GN=ECH1 PE=1 SV=2

40	Spectrin beta chain, non-erythrocytic 1 OS=Homo sapiens GN=SPTBN1 PE=1 SV=2
41	40S ribosomal protein S27-like OS=Homo sapiens GN=RPS27L PE=1 SV=3
42	40S ribosomal protein S14 OS=Homo sapiens GN=RPS14 PE=1 SV=3
43	ATP synthase subunit alpha, mitochondrial OS=Homo sapiens GN=ATP5A1 PE=1 SV=1
44	Prohibitin OS=Homo sapiens GN=PHB PE=1 SV=1
45	60S ribosomal protein L15 OS=Homo sapiens GN=RPL15 PE=1 SV=2
46	Protein phosphatase 1G OS=Homo sapiens GN=PPM1G PE=1 SV=1
47	Glyceraldehyde-3-phosphate dehydrogenase OS=Homo sapiens GN=GAPDH PE=1 SV=3
48	Peptidyl-prolyl cis-trans isomerase FKBP4 OS=Homo sapiens GN=FKBP4 PE=1 SV=3
49	Peptidyl-prolyl cis-trans isomerase B OS=Homo sapiens GN=PPIB PE=1 SV=2
50	Proliferation-associated protein 2G4 OS=Homo sapiens GN=PA2G4 PE=1 SV=3
51	Ras GTPase-activating protein-binding protein 2 OS=Homo sapiens GN=G3BP2 PE=1 SV=2
52	T-complex protein 1 subunit theta OS=Homo sapiens GN=CCT8 PE=1 SV=4
53	Catalase OS=Homo sapiens GN=CAT PE=1 SV=3
54	Histone H4 OS=Homo sapiens GN=HIST1H4A PE=1 SV=2
55	Nuclear autoantigenic sperm protein OS=Homo sapiens GN=NASP PE=1 SV=2
56	Integrin beta-1 OS=Homo sapiens GN=ITGB1 PE=1 SV=2
57	Heterogeneous nuclear ribonucleoprotein K OS=Homo sapiens GN=HNRNPK PE=1 SV=1
58	NSFL1 cofactor p47 OS=Homo sapiens GN=NSFL1C PE=1 SV=2
59	Calcium-regulated heat stable protein 1 OS=Homo sapiens GN=CARHSP1 PE=1 SV=2
60	Eukaryotic initiation factor 4A-I OS=Homo sapiens GN=EIF4A1 PE=1 SV=1
61	Endoplasmin OS=Homo sapiens GN=HSP90B1 PE=1 SV=1
62	Hematological and neurological expressed 1 protein OS=Homo sapiens GN=HN1 PE=1 SV=3
63	Peptidyl-prolyl cis-trans isomerase A OS=Homo sapiens GN=PPIA PE=1 SV=2
64	Spectrin alpha chain, non-erythrocytic 1 OS=Homo sapiens GN=SPTAN1 PE=1 SV=3
65	Poly(rC)-binding protein 1 OS=Homo sapiens GN=PCBP1 PE=1 SV=2
66	G-rich sequence factor 1 OS=Homo sapiens GN=GRSF1 PE=1 SV=3
67	LIM and SH3 domain protein 1 OS=Homo sapiens GN=LASP1 PE=1 SV=2
68	60S ribosomal protein L22 OS=Homo sapiens GN=RPL22 PE=1 SV=2
69	Perilipin-3 OS=Homo sapiens GN=PLIN3 PE=1 SV=3
70	Heterogeneous nuclear ribonucleoprotein A0 OS=Homo sapiens GN=HNRNPA0 PE=1 SV=1
71	ATP synthase subunit beta, mitochondrial OS=Homo sapiens GN=ATP5B PE=1 SV=3
72	Histone H1.4 OS=Homo sapiens GN=HIST1H1E PE=1 SV=2
73	Pyruvate kinase PKM OS=Homo sapiens GN=PKM PE=1 SV=4
74	MARCKS-related protein OS=Homo sapiens GN=MARCKSL1 PE=1 SV=2
75	Citrate synthase, mitochondrial OS=Homo sapiens GN=CS PE=1 SV=2
76	60S ribosomal protein L32 OS=Homo sapiens GN=RPL32 PE=1 SV=2
77	Elongation factor Tu, mitochondrial OS=Homo sapiens GN=TUFM PE=1 SV=2
78	Basigin OS=Homo sapiens GN=BSG PE=1 SV=2
79	Elongation factor 2 OS=Homo sapiens GN=EEF2 PE=1 SV=4
80	T-complex protein 1 subunit delta OS=Homo sapiens GN=CCT4 PE=1 SV=4
81	60S ribosomal protein L23a OS=Homo sapiens GN=RPL23A PE=1 SV=1
82	Nucleophosmin OS=Homo sapiens GN=NPM1 PE=1 SV=2
83	Tubulin beta chain OS=Homo sapiens GN=TUBB PE=1 SV=2
84	T-complex protein 1 subunit beta OS=Homo sapiens GN=CCT2 PE=1 SV=4

Table S1 Identified protein list for Hep G2 cell lysate. The protein with the highest protein score is hit number 1 and so on.

	SiNPs - Hep G2 cell lysate
1	Keratin, type II cytoskeletal 1 OS=Homo sapiens GN=KRT1 PE=1 SV=6
2	Actin, cytoplasmic 1 OS=Homo sapiens GN=ACTB PE=1 SV=1
3	Keratin, type I cytoskeletal 9 OS=Homo sapiens GN=KRT9 PE=1 SV=3
4	Keratin, type I cytoskeletal 10 OS=Homo sapiens GN=KRT10 PE=1 SV=6
5	Tubulin beta chain OS=Homo sapiens GN=TUBB PE=1 SV=2
6	Tubulin alpha-1B chain OS=Homo sapiens GN=TUBA1B PE=1 SV=1
7	Myosin-9 OS=Homo sapiens GN=MYH9 PE=1 SV=4
8	Elongation factor 1-alpha 1 OS=Homo sapiens GN=EEF1A1 PE=1 SV=1
9	Pyruvate kinase PKM OS=Homo sapiens GN=PKM PE=1 SV=4
10	Peptidyl-prolyl cis-trans isomerase A OS=Homo sapiens GN=PPIA PE=1 SV=2
11	L-lactate dehydrogenase A chain OS=Homo sapiens GN=LDHA PE=1 SV=2
12	Glyceraldehyde-3-phosphate dehydrogenase OS=Homo sapiens GN=GAPDH PE=1 SV=3
13	Heat shock protein HSP 90-beta OS=Homo sapiens GN=HSP90AB1 PE=1 SV=4
14	Alpha-enolase OS=Homo sapiens GN=ENO1 PE=1 SV=2
15	78 kDa glucose-regulated protein OS=Homo sapiens GN=HSPA5 PE=1 SV=2
16	60 kDa heat shock protein, mitochondrial OS=Homo sapiens GN=HSPD1 PE=1 SV=2
17	Malate dehydrogenase, mitochondrial OS=Homo sapiens GN=MDH2 PE=1 SV=3
18	Cofilin-1 OS=Homo sapiens GN=CFL1 PE=1 SV=3
19	Radixin OS=Homo sapiens GN=RDX PE=1 SV=1
20	Histone H2A type 1-B/E OS=Homo sapiens GN=HIST1H2AB PE=1 SV=2
21	Triosephosphate isomerase OS=Homo sapiens GN=TPI1 PE=1 SV=3
22	Profilin-1 OS=Homo sapiens GN=PFN1 PE=1 SV=2
23	Serpin H1 OS=Homo sapiens GN=SERPINH1 PE=1 SV=2
24	Heterogeneous nuclear ribonucleoprotein K OS=Homo sapiens GN=HNRNPK PE=1 SV=1
25	14-3-3 protein zeta/delta OS=Homo sapiens GN=YWHAZ PE=1 SV=1
26	Vinculin OS=Homo sapiens GN=VCL PE=1 SV=4
27	Fructose-bisphosphate aldolase A OS=Homo sapiens GN=ALDOA PE=1 SV=2
28	Heterogeneous nuclear ribonucleoprotein U OS=Homo sapiens GN=HNRNPU PE=1 SV=6
29	Vimentin OS=Homo sapiens GN=VIM PE=1 SV=4
30	10 kDa heat shock protein, mitochondrial OS=Homo sapiens GN=HSPE1 PE=1 SV=2
31	Signal recognition particle 14 kDa protein OS=Homo sapiens GN=SRP14 PE=1 SV=2
32	Calreticulin OS=Homo sapiens GN=CALR PE=1 SV=1
33	Nascent polypeptide-associated complex subunit alpha, muscle-specific form OS=Homo sapiens GN=NACA PE=1 SV=1
34	60S ribosomal protein L22 OS=Homo sapiens GN=RPL22 PE=1 SV=2
35	Protein disulfide-isomerase A4 OS=Homo sapiens GN=PDIA4 PE=1 SV=2
36	Thioredoxin OS=Homo sapiens GN=TXN PE=1 SV=3
37	Histone H1t OS=Homo sapiens GN=HIST1H1T PE=2 SV=4
38	Phosphoglycerate mutase 1 OS=Homo sapiens GN=PGAM1 PE=1 SV=2
39	Eukaryotic translation initiation factor 5B OS=Homo sapiens GN=EIF5B PE=1 SV=4
40	Far upstream element-binding protein 2 OS=Homo sapiens GN=KHSRP PE=1 SV=4
41	40S ribosomal protein SA OS=Homo sapiens GN=RPSA PE=1 SV=4
42	Myosin light chain 6B OS=Homo sapiens GN=MYL6B PE=1 SV=1
43	Dermcidin OS=Homo sapiens GN=DCD PE=1 SV=2
44	Glutathione S-transferase P OS=Homo sapiens GN=GSTP1 PE=1 SV=2

45	Elongation factor 2 OS=Homo sapiens GN=EEF2 PE=1 SV=4
46	Phosphoglycerate kinase 1 OS=Homo sapiens GN=PGK1 PE=1 SV=3
47	Small nuclear ribonucleoprotein Sm D3 OS=Homo sapiens GN=SNRPD3 PE=1 SV=1
48	Protein disulfide-isomerase A6 OS=Homo sapiens GN=PDIA6 PE=1 SV=1
49	Caldesmon OS=Homo sapiens GN=CALD1 PE=1 SV=3
50	Moesin OS=Homo sapiens GN=MSN PE=1 SV=3
51	Kinesin-1 heavy chain OS=Homo sapiens GN=KIF5B PE=1 SV=1
52	Parathymosin OS=Homo sapiens GN=PTMS PE=1 SV=2
53	Annexin A5 OS=Homo sapiens GN=ANXA5 PE=1 SV=2
54	Histone H4 OS=Homo sapiens GN=HIST1H4A PE=1 SV=2
55	Tropomyosin beta chain OS=Homo sapiens GN=TPM2 PE=1 SV=1
56	Putative high mobility group protein B1-like 1 OS=Homo sapiens GN=HMGB1P1 PE=5 SV=1
56	Nuclear autoantigen Sp-100 OS=Homo sapiens GN=SP100 PE=1 SV=3
57	Eukaryotic initiation factor 4A-I OS=Homo sapiens GN=EIF4A1 PE=1 SV=1
58	Chloride intracellular channel protein 1 OS=Homo sapiens GN=CLIC1 PE=1 SV=4
59	Protein S100-A11 OS=Homo sapiens GN=S100A11 PE=1 SV=2
60	C-1-tetrahydrofolate synthase, cytoplasmic OS=Homo sapiens GN=MTHFD1 PE=1 SV=3
61	14-3-3 protein gamma OS=Homo sapiens GN=YWHAG PE=1 SV=2
62	ATP synthase subunit alpha, mitochondrial OS=Homo sapiens GN=ATP5A1 PE=1 SV=1
63	Ubiquitin-conjugating enzyme E2 N OS=Homo sapiens GN=UBE2N PE=1 SV=1
64	Adenylosuccinate lyase OS=Homo sapiens GN=ADSL PE=1 SV=2
65	Endothelial differentiation-related factor 1 OS=Homo sapiens GN=EDF1 PE=1 SV=1
66	Histone H2B type 1-B OS=Homo sapiens GN=HIST1H2BB PE=1 SV=2
67	Histone H3.3C OS=Homo sapiens GN=H3F3C PE=1 SV=3
68	Profilin-2 OS=Homo sapiens GN=PFN2 PE=1 SV=3
69	Malate dehydrogenase, cytoplasmic OS=Homo sapiens GN=MDH1 PE=1 SV=4
70	Stress-70 protein, mitochondrial OS=Homo sapiens GN=HSPA9 PE=1 SV=2
71	Ubiquitin-associated protein 2-like OS=Homo sapiens GN=UBAP2L PE=1 SV=2
72	Plasminogen activator inhibitor 1 RNA-binding protein OS=Homo sapiens GN=SERBP1 PE=1 SV=2
73	Filamin-A OS=Homo sapiens GN=FLNA PE=1 SV=4
74	GTP-binding nuclear protein Ran OS=Homo sapiens GN=RAN PE=1 SV=3
75	Nucleophosmin OS=Homo sapiens GN=NPM1 PE=1 SV=2

Table S2 Identified protein list from the protein corona of SiNPs exposed to Hep G2 cell lysate. The protein with the highest protein score is hit number 1 and so on.

	AuNPs - Hep G2 cell lysate
1	Keratin, type I cytoskeletal 9 OS=Homo sapiens GN=KRT9 PE=1 SV=3
2	Keratin, type II cytoskeletal 1 OS=Homo sapiens GN=KRT1 PE=1 SV=6
3	Desmoplakin OS=Homo sapiens GN=DSP PE=1 SV=3
4	14-3-3 protein zeta/delta OS=Homo sapiens GN=YWHAZ PE=1 SV=1
5	60 kDa heat shock protein, mitochondrial OS=Homo sapiens GN=HSPD1 PE=1 SV=2
6	Peptidyl-prolyl cis-trans isomerase A OS=Homo sapiens GN=PPIA PE=1 SV=2
7	Actin, cytoplasmic 1 OS=Homo sapiens GN=ACTB PE=1 SV=1

8	14-3-3 protein epsilon OS=Homo sapiens GN=YWHAE PE=1 SV=1
9	L-lactate dehydrogenase A chain OS=Homo sapiens GN=LDHA PE=1 SV=2
10	Alpha-enolase OS=Homo sapiens GN=ENO1 PE=1 SV=2
11	Ubiquitin-like modifier-activating enzyme 1 OS=Homo sapiens GN=UBA1 PE=1 SV=3
12	Desmoglein-1 OS=Homo sapiens GN=DSG1 PE=1 SV=2
13	Elongation factor 2 OS=Homo sapiens GN=EEF2 PE=1 SV=4
14	Protein S100-A11 OS=Homo sapiens GN=S100A11 PE=1 SV=2
15	Dermcidin OS=Homo sapiens GN=DCD PE=1 SV=2
16	Vinculin OS=Homo sapiens GN=VCL PE=1 SV=4
17	Lactoylglutathione lyase OS=Homo sapiens GN=GLO1 PE=1 SV=4
18	Junction plakoglobin OS=Homo sapiens GN=JUP PE=1 SV=3
19	14-3-3 protein beta/alpha OS=Homo sapiens GN=YWHAB PE=1 SV=3
20	Rab GDP dissociation inhibitor beta OS=Homo sapiens GN=GDI2 PE=1 SV=2
21	Tubulin alpha-1B chain OS=Homo sapiens GN=TUBA1B PE=1 SV=1
22	Glyceraldehyde-3-phosphate dehydrogenase OS=Homo sapiens GN=GAPDH PE=1 SV=3
23	Dermokine OS=Homo sapiens GN=DMKN PE=1 SV=3
24	Cytochrome c OS=Homo sapiens GN=CYCS PE=1 SV=2
25	Glucose-6-phosphate isomerase OS=Homo sapiens GN=GPI PE=1 SV=4
26	Pyruvate kinase PKM OS=Homo sapiens GN=PKM PE=1 SV=4
27	L-lactate dehydrogenase B chain OS=Homo sapiens GN=LDHB PE=1 SV=2
28	Heat shock protein HSP 90-beta OS=Homo sapiens GN=HSP90AB1 PE=1 SV=4
29	Fatty acid-binding protein, epidermal OS=Homo sapiens GN=FABP5 PE=1 SV=3
30	Calmodulin-like protein 5 OS=Homo sapiens GN=CALML5 PE=1 SV=2
31	Hornerin OS=Homo sapiens GN=HRNR PE=1 SV=2
32	Acidic leucine-rich nuclear phosphoprotein 32 family member E OS=Homo sapiens GN=ANP32E PE=1 SV=1
33	14-3-3 protein theta OS=Homo sapiens GN=YWHAQ PE=1 SV=1

Table S3 Identified protein list from the protein corona of AuNPs exposed to Hep G2 cell lysate. The protein with the highest protein score is hit number 1 and so on.

	A 2780 cell lysate
1	Alpha-enolase OS=Homo sapiens GN=ENO1 PE=1 SV=2
2	60 kDa heat shock protein, mitochondrial OS=Homo sapiens GN=HSPD1 PE=1 SV=2
3	Ubiquitin-like modifier-activating enzyme 1 OS=Homo sapiens GN=UBA1 PE=1 SV=3
4	Actin, cytoplasmic 1 OS=Homo sapiens GN=ACTB PE=1 SV=1
5	Heat shock cognate 71 kDa protein OS=Homo sapiens GN=HSPA8 PE=1 SV=1
6	Elongation factor 2 OS=Homo sapiens GN=EEF2 PE=1 SV=4
7	Heat shock protein HSP 90-beta OS=Homo sapiens GN=HSP90AB1 PE=1 SV=4
8	Calreticulin OS=Homo sapiens GN=CALR PE=1 SV=1
9	Pyruvate kinase PKM OS=Homo sapiens GN=PKM PE=1 SV=4
10	Glyceraldehyde-3-phosphate dehydrogenase OS=Homo sapiens GN=GAPDH PE=1 SV=3
11	Profilin-1 OS=Homo sapiens GN=PFN1 PE=1 SV=2

12	Malate dehydrogenase, mitochondrial OS=Homo sapiens GN=MDH2 PE=1 SV=3
13	Stress-70 protein, mitochondrial OS=Homo sapiens GN=HSPA9 PE=1 SV=2
14	Tubulin beta chain OS=Homo sapiens GN=TUBB PE=1 SV=2
15	Phosphoglycerate kinase 1 OS=Homo sapiens GN=PGK1 PE=1 SV=3
16	Glutathione S-transferase P OS=Homo sapiens GN=GSTP1 PE=1 SV=2
17	Glucose-6-phosphate isomerase OS=Homo sapiens GN=GPI PE=1 SV=4
18	Heat shock 70 kDa protein 4 OS=Homo sapiens GN=HSPA4 PE=1 SV=4
19	14-3-3 protein zeta/delta OS=Homo sapiens GN=YWHAZ PE=1 SV=1
20	Tubulin alpha-1B chain OS=Homo sapiens GN=TUBA1B PE=1 SV=1
21	Lupus La protein OS=Homo sapiens GN=SSB PE=1 SV=2
22	Rab GDP dissociation inhibitor beta OS=Homo sapiens GN=GDI2 PE=1 SV=2
23	ATP synthase subunit beta, mitochondrial OS=Homo sapiens GN=ATP5B PE=1 SV=3
24	Fructose-bisphosphate aldolase A OS=Homo sapiens GN=ALDOA PE=1 SV=2
25	Hypoxia up-regulated protein 1 OS=Homo sapiens GN=HYOU1 PE=1 SV=1
26	Protein disulfide-isomerase A4 OS=Homo sapiens GN=PDIA4 PE=1 SV=2
27	Protein disulfide-isomerase A6 OS=Homo sapiens GN=PDIA6 PE=1 SV=1
28	L-lactate dehydrogenase A chain OS=Homo sapiens GN=LDHA PE=1 SV=2
29	Serpin H1 OS=Homo sapiens GN=SERPINH1 PE=1 SV=2
30	Triosephosphate isomerase OS=Homo sapiens GN=TPI1 PE=1 SV=3
31	Phosphoglycerate mutase 1 OS=Homo sapiens GN=PGAM1 PE=1 SV=2
32	Annexin A6 OS=Homo sapiens GN=ANXA6 PE=1 SV=3
33	Cofilin-1 OS=Homo sapiens GN=CFL1 PE=1 SV=3
34	Vinculin OS=Homo sapiens GN=VCL PE=1 SV=4
35	Importin subunit beta-1 OS=Homo sapiens GN=KPNB1 PE=1 SV=2
36	Nucleoside diphosphate kinase B OS=Homo sapiens GN=NME2 PE=1 SV=1
37	Annexin A2 OS=Homo sapiens GN=ANXA2 PE=1 SV=2
38	Bifunctional purine biosynthesis protein PURH OS=Homo sapiens GN=ATIC PE=1 SV=3
39	Peptidyl-prolyl cis-trans isomerase A OS=Homo sapiens GN=PPIA PE=1 SV=2
40	Alanine--tRNA ligase, cytoplasmic OS=Homo sapiens GN=AARS PE=1 SV=2
41	Peroxiredoxin-6 OS=Homo sapiens GN=PRDX6 PE=1 SV=3
42	Elongation factor 1-alpha 1 OS=Homo sapiens GN=EEF1A1 PE=1 SV=1
43	Moesin OS=Homo sapiens GN=MSN PE=1 SV=3
44	Stress-induced-phosphoprotein 1 OS=Homo sapiens GN=STIP1 PE=1 SV=1
45	Nucleolin OS=Homo sapiens GN=NCL PE=1 SV=3
46	Transketolase OS=Homo sapiens GN=TKT PE=1 SV=3
47	Lactoylglutathione lyase OS=Homo sapiens GN=GLO1 PE=1 SV=4
48	Acidic leucine-rich nuclear phosphoprotein 32 family member E OS=Homo sapiens GN=ANP32E PE=1 SV=1
49	Adenosylhomocysteinase OS=Homo sapiens GN=AHCY PE=1 SV=4
50	Vimentin OS=Homo sapiens GN=VIM PE=1 SV=4
51	Gelsolin OS=Homo sapiens GN=GSN PE=1 SV=1
52	Protein disulfide-isomerase OS=Homo sapiens GN=P4HB PE=1 SV=3
53	Alpha-actinin-4 OS=Homo sapiens GN=ACTN4 PE=1 SV=2
54	Heterogeneous nuclear ribonucleoprotein K OS=Homo sapiens GN=HNRNPK PE=1 SV=1
55	Prolyl endopeptidase OS=Homo sapiens GN=PREP PE=1 SV=2
56	Eukaryotic initiation factor 4A-I OS=Homo sapiens GN=EIF4A1 PE=1 SV=1
57	Obg-like ATPase 1 OS=Homo sapiens GN=OLA1 PE=1 SV=2
58	Chloride intracellular channel protein 1 OS=Homo sapiens GN=CLIC1 PE=1 SV=4

59	Nucleophosmin OS=Homo sapiens GN=NPM1 PE=1 SV=2
60	Nascent polypeptide-associated complex subunit alpha, muscle-specific form OS=Homo sapiens GN=NACA PE=1 SV=1
61	Adenosine kinase OS=Homo sapiens GN=ADK PE=1 SV=2
62	Protein S100-A11 OS=Homo sapiens GN=S100A11 PE=1 SV=2
63	Tropomyosin alpha-4 chain OS=Homo sapiens GN=TPM4 PE=1 SV=3
64	Coactosin-like protein OS=Homo sapiens GN=COTL1 PE=1 SV=3
65	Transitional endoplasmic reticulum ATPase OS=Homo sapiens GN=VCP PE=1 SV=4
66	Phosphoribosylformylglycinamidine synthase OS=Homo sapiens GN=PFAS PE=1 SV=4
67	Protein deglycase DJ-1 OS=Homo sapiens GN=PARK7 PE=1 SV=2
68	Aconitate hydratase, mitochondrial OS=Homo sapiens GN=ACO2 PE=1 SV=2
69	Phosphatidylethanolamine-binding protein 1 OS=Homo sapiens GN=PEBP1 PE=1 SV=3
70	Peptidyl-prolyl cis-trans isomerase FKBP10 OS=Homo sapiens GN=FKBP10 PE=1 SV=1
71	Nucleosome assembly protein 1-like 1 OS=Homo sapiens GN=NAP1L1 PE=1 SV=1
72	Prostaglandin reductase 1 OS=Homo sapiens GN=PTGR1 PE=1 SV=2
73	Leucine-rich PPR motif-containing protein, mitochondrial OS=Homo sapiens GN=LRPPRC PE=1 SV=3
74	S-formylglutathione hydrolase OS=Homo sapiens GN=ESD PE=1 SV=2
75	KDEL motif-containing protein 2 OS=Homo sapiens GN=KDELC2 PE=1 SV=2
76	Complement component 1 Q subcomponent-binding protein, mitochondrial OS=Homo sapiens GN=C1QBP PE=1 SV=1
77	Cytochrome c OS=Homo sapiens GN=CYCS PE=1 SV=2
78	Nuclear autoantigenic sperm protein OS=Homo sapiens GN=NASP PE=1 SV=2
79	Fermitin family homolog 2 OS=Homo sapiens GN=FERMT2 PE=1 SV=1
80	Annexin A5 OS=Homo sapiens GN=ANXA5 PE=1 SV=2
81	40S ribosomal protein SA OS=Homo sapiens GN=RPSA PE=1 SV=4
82	Flavin reductase (NADPH) OS=Homo sapiens GN=BLVRB PE=1 SV=3
83	Malignant T-cell-amplified sequence 1 OS=Homo sapiens GN=MCTS1 PE=1 SV=1
84	Purine nucleoside phosphorylase OS=Homo sapiens GN=PNP PE=1 SV=2
85	Transgelin-2 OS=Homo sapiens GN=TAGLN2 PE=1 SV=3
86	Glutathione S-transferase theta-2 OS=Homo sapiens GN=GSTT2 PE=1 SV=1
87	Peroxiredoxin-5, mitochondrial OS=Homo sapiens GN=PRDX5 PE=1 SV=4
88	Tyrosine--tRNA ligase, cytoplasmic OS=Homo sapiens GN=YARS PE=1 SV=4
89	Prefoldin subunit 5 OS=Homo sapiens GN=PFDN5 PE=1 SV=2
90	Protein dpy-30 homolog OS=Homo sapiens GN=DPY30 PE=1 SV=1
91	Protein disulfide-isomerase A3 OS=Homo sapiens GN=PDIA3 PE=1 SV=4
92	6-phosphogluconate dehydrogenase, decarboxylating OS=Homo sapiens GN=PGD PE=1 SV=3
93	Protein phosphatase 1 regulatory subunit 7 OS=Homo sapiens GN=PPP1R7 PE=1 SV=1
94	Peroxiredoxin-2 OS=Homo sapiens GN=PRDX2 PE=1 SV=5
95	UPF0160 protein MYG1, mitochondrial OS=Homo sapiens GN=C12orf10 PE=1 SV=2
96	Heat shock protein beta-1 OS=Homo sapiens GN=HSPB1 PE=1 SV=2
97	Prothymosin alpha OS=Homo sapiens GN=PTMA PE=1 SV=2
98	Filamin-A OS=Homo sapiens GN=FLNA PE=1 SV=4
99	Transaldolase OS=Homo sapiens GN=TALDO1 PE=1 SV=2
100	Hsc70-interacting protein OS=Homo sapiens GN=ST13 PE=1 SV=2
101	Glucosamine 6-phosphate N-acetyltransferase OS=Homo sapiens GN=GNPNAT1 PE=1 SV=1
102	Calmodulin OS=Homo sapiens GN=CALM1 PE=1 SV=2
103	Glycine--tRNA ligase OS=Homo sapiens GN=GARS PE=1 SV=3
104	Delta(3,5)-Delta(2,4)-dienoyl-CoA isomerase, mitochondrial OS=Homo sapiens GN=ECH1 PE=1

	SV=2
105	Isocitrate dehydrogenase [NADP] cytoplasmic OS=Homo sapiens GN=IDH1 PE=1 SV=2
106	ATP synthase subunit alpha, mitochondrial OS=Homo sapiens GN=ATP5A1 PE=1 SV=1
107	Nucleosome assembly protein 1-like 4 OS=Homo sapiens GN=NAP1L4 PE=1 SV=1
108	Endoplasmic reticulum resident protein 29 OS=Homo sapiens GN=ERP29 PE=1 SV=4
109	Serine/threonine-protein kinase 26 OS=Homo sapiens GN=STK26 PE=1 SV=2
110	Dynamin-1-like protein OS=Homo sapiens GN=DNM1L PE=1 SV=2
111	Retinal dehydrogenase 1 OS=Homo sapiens GN=ALDH1A1 PE=1 SV=2
112	Carbonyl reductase [NADPH] 3 OS=Homo sapiens GN=CBR3 PE=1 SV=3
113	Thioredoxin OS=Homo sapiens GN=TXN PE=1 SV=3
114	Tryptophan--tRNA ligase, cytoplasmic OS=Homo sapiens GN=WARS PE=1 SV=2
115	Adenine phosphoribosyltransferase OS=Homo sapiens GN=APRT PE=1 SV=2
116	Programmed cell death 6-interacting protein OS=Homo sapiens GN=PDCD6IP PE=1 SV=1
117	Eukaryotic translation initiation factor 4H OS=Homo sapiens GN=EIF4H PE=1 SV=5
118	BRCA2 and CDKN1A-interacting protein OS=Homo sapiens GN=BCCIP PE=1 SV=1
119	Importin-5 OS=Homo sapiens GN=IPO5 PE=1 SV=4
120	Prostaglandin E synthase 3 OS=Homo sapiens GN=PTGES3 PE=1 SV=1
121	Histone H2B type 1-B OS=Homo sapiens GN=HIST1H2BB PE=1 SV=2
122	Talin-1 OS=Homo sapiens GN=TLN1 PE=1 SV=3
123	Importin-9 OS=Homo sapiens GN=IPO9 PE=1 SV=3
124	Fructose-2,6-bisphosphatase TIGAR OS=Homo sapiens GN=TIGAR PE=1 SV=1
125	DNA-(apurinic or apyrimidinic site) lyase OS=Homo sapiens GN=APEX1 PE=1 SV=2
126	Histone H2A type 1-B/E OS=Homo sapiens GN=HIST1H2AB PE=1 SV=2
127	F-actin-capping protein subunit alpha-1 OS=Homo sapiens GN=CAPZA1 PE=1 SV=3
128	D-3-phosphoglycerate dehydrogenase OS=Homo sapiens GN=PHGDH PE=1 SV=4
129	10 kDa heat shock protein, mitochondrial OS=Homo sapiens GN=HSPE1 PE=1 SV=2
130	Nestin OS=Homo sapiens GN=NES PE=1 SV=2
131	Protein SET OS=Homo sapiens GN=SET PE=1 SV=3
132	Plastin-3 OS=Homo sapiens GN=PLS3 PE=1 SV=4
133	Exportin-1 OS=Homo sapiens GN=XPO1 PE=1 SV=1
134	Elongation factor 1-beta OS=Homo sapiens GN=EEF1B2 PE=1 SV=3
135	Translin-associated protein X OS=Homo sapiens GN=TSNAX PE=1 SV=1
136	Staphylococcal nuclease domain-containing protein 1 OS=Homo sapiens GN=SND1 PE=1 SV=1
137	X-ray repair cross-complementing protein 5 OS=Homo sapiens GN=XRCC5 PE=1 SV=3
138	Collagen alpha-1(III) chain OS=Homo sapiens GN=COL3A1 PE=1 SV=4
139	Acidic leucine-rich nuclear phosphoprotein 32 family member B OS=Homo sapiens GN=ANP32B PE=1 SV=1
140	Activated RNA polymerase II transcriptional coactivator p15 OS=Homo sapiens GN=SUB1 PE=1 SV=3
141	Aspartate aminotransferase, cytoplasmic OS=Homo sapiens GN=GOT1 PE=1 SV=3
142	Sepiapterin reductase OS=Homo sapiens GN=SPR PE=1 SV=1
143	Calponin-2 OS=Homo sapiens GN=CNN2 PE=1 SV=4
144	Nucleoprotein TPR OS=Homo sapiens GN=TPR PE=1 SV=3
145	Glutathione S-transferase omega-1 OS=Homo sapiens GN=GSTO1 PE=1 SV=2
146	Annexin A4 OS=Homo sapiens GN=ANXA4 PE=1 SV=4
147	Importin subunit alpha-3 OS=Homo sapiens GN=KPNA4 PE=1 SV=1
148	S-methyl-5~-thioadenosine phosphorylase OS=Homo sapiens GN=MTAP PE=1 SV=2
149	Maleylacetoacetate isomerase OS=Homo sapiens GN=GSTZ1 PE=1 SV=3
150	Inorganic pyrophosphatase OS=Homo sapiens GN=PPA1 PE=1 SV=2

151	Dipeptidyl peptidase 3 OS=Homo sapiens GN=DPP3 PE=1 SV=2
152	Prefoldin subunit 3 OS=Homo sapiens GN=VBP1 PE=1 SV=3
153	Electron transfer flavoprotein subunit alpha, mitochondrial OS=Homo sapiens GN=ETFA PE=1 SV=1
154	Proliferating cell nuclear antigen OS=Homo sapiens GN=PCNA PE=1 SV=1
155	Dihydrofolate reductase OS=Homo sapiens GN=DHFR PE=1 SV=2
156	Porphobilinogen deaminase OS=Homo sapiens GN=HMBS PE=1 SV=2
157	Protein phosphatase 1F OS=Homo sapiens GN=PPM1F PE=1 SV=3
158	60 kDa SS-A/Ro ribonucleoprotein OS=Homo sapiens GN=TROVE2 PE=1 SV=2
159	NAD-dependent malic enzyme, mitochondrial OS=Homo sapiens GN=ME2 PE=1 SV=1
160	Superoxide dismutase [Cu-Zn] OS=Homo sapiens GN=SOD1 PE=1 SV=2
161	Myosin light polypeptide 6 OS=Homo sapiens GN=MYL6 PE=1 SV=2
162	Microtubule-associated protein 4 OS=Homo sapiens GN=MAP4 PE=1 SV=3
163	Translationally-controlled tumor protein OS=Homo sapiens GN=TPT1 PE=1 SV=1
164	Trifunctional purine biosynthetic protein adenosine-3 OS=Homo sapiens GN=GART PE=1 SV=1
165	Protein S100-A13 OS=Homo sapiens GN=S100A13 PE=1 SV=1
166	3-hydroxyacyl-CoA dehydrogenase type-2 OS=Homo sapiens GN=HSD17B10 PE=1 SV=3
167	Cytosolic non-specific dipeptidase OS=Homo sapiens GN=CNDP2 PE=1 SV=2
168	Glucosidase 2 subunit beta OS=Homo sapiens GN=PRKCSH PE=1 SV=2
169	Transcription factor BTF3 OS=Homo sapiens GN=BTF3 PE=1 SV=1
170	Ubiquitin carboxyl-terminal hydrolase 14 OS=Homo sapiens GN=USP14 PE=1 SV=3
171	Macrophage migration inhibitory factor OS=Homo sapiens GN=MIF PE=1 SV=4
172	Glutaredoxin-3 OS=Homo sapiens GN=GLRX3 PE=1 SV=2
173	Hypoxanthine-guanine phosphoribosyltransferase OS=Homo sapiens GN=HPRT1 PE=1 SV=2
174	Malate dehydrogenase, cytoplasmic OS=Homo sapiens GN=MDH1 PE=1 SV=4
175	Acetyl-CoA acetyltransferase, mitochondrial OS=Homo sapiens GN=ACAT1 PE=1 SV=1
176	Isocitrate dehydrogenase [NAD] subunit beta, mitochondrial OS=Homo sapiens GN=IDH3B PE=1 SV=2
177	Poly(rC)-binding protein 1 OS=Homo sapiens GN=PCBP1 PE=1 SV=2
178	Glycylpeptide N-tetradecanoyltransferase 1 OS=Homo sapiens GN=NMT1 PE=1 SV=2
179	Glyoxalase domain-containing protein 4 OS=Homo sapiens GN=GLOD4 PE=1 SV=1
180	Chromobox protein homolog 3 OS=Homo sapiens GN=CBX3 PE=1 SV=4
181	Proteasome activator complex subunit 3 OS=Homo sapiens GN=PSME3 PE=1 SV=1
182	Phosphoglucomutase-1 OS=Homo sapiens GN=PGM1 PE=1 SV=3
183	Vitronectin OS=Homo sapiens GN=VTN PE=1 SV=1
184	Single-stranded DNA-binding protein, mitochondrial OS=Homo sapiens GN=SSBP1 PE=1 SV=1
185	WD repeat-containing protein 61 OS=Homo sapiens GN=WDR61 PE=1 SV=1
186	Peptidyl-prolyl cis-trans isomerase FKBP4 OS=Homo sapiens GN=FKBP4 PE=1 SV=3
187	Glycine cleavage system H protein, mitochondrial OS=Homo sapiens GN=GCSH PE=1 SV=2
188	Ubiquitin carboxyl-terminal hydrolase isozyme L3 OS=Homo sapiens GN=UCHL3 PE=1 SV=1
189	X-ray repair cross-complementing protein 6 OS=Homo sapiens GN=XRCC6 PE=1 SV=2
190	SH3 domain-binding glutamic acid-rich-like protein OS=Homo sapiens GN=SH3BGRL PE=1 SV=1
191	Alcohol dehydrogenase [NADP(+)] OS=Homo sapiens GN=AKR1A1 PE=1 SV=3
192	Proline synthase co-transcribed bacterial homolog protein OS=Homo sapiens GN=PROSC PE=1 SV=1
193	Protein phosphatase 1G OS=Homo sapiens GN=PPM1G PE=1 SV=1
194	NADP-dependent malic enzyme OS=Homo sapiens GN=ME1 PE=1 SV=1
195	Xaa-Pro dipeptidase OS=Homo sapiens GN=PEPD PE=1 SV=3
196	Platelet-activating factor acetylhydrolase IB subunit beta OS=Homo sapiens GN=PAFAH1B2 PE=1

	SV=1
197	Neutral alpha-glucosidase AB OS=Homo sapiens GN=GANAB PE=1 SV=3
198	Ras-related protein Rab-1A OS=Homo sapiens GN=RAB1A PE=1 SV=3
199	Hydroxysteroid dehydrogenase-like protein 2 OS=Homo sapiens GN=HSDL2 PE=1 SV=1
200	Cysteine and histidine-rich domain-containing protein 1 OS=Homo sapiens GN=CHORDC1 PE=1 SV=2
201	Exportin-2 OS=Homo sapiens GN=CSE1L PE=1 SV=3
202	ADP-sugar pyrophosphatase OS=Homo sapiens GN=NUDT5 PE=1 SV=1
203	Proteasome activator complex subunit 2 OS=Homo sapiens GN=PSME2 PE=1 SV=4
204	Succinyl-CoA ligase [GDP-forming] subunit beta, mitochondrial OS=Homo sapiens GN=SUCLG2 PE=1 SV=2
205	SUMO-activating enzyme subunit 2 OS=Homo sapiens GN=UBA2 PE=1 SV=2
206	Tubulin-specific chaperone A OS=Homo sapiens GN=TBCA PE=1 SV=3
207	Apoptosis inhibitor 5 OS=Homo sapiens GN=API5 PE=1 SV=3
208	Alpha-ketoglutarate-dependent dioxygenase FTO OS=Homo sapiens GN=FTO PE=1 SV=3
209	Visinin-like protein 1 OS=Homo sapiens GN=VSNL1 PE=1 SV=2
210	GTP-binding nuclear protein Ran OS=Homo sapiens GN=RAN PE=1 SV=3
211	Multifunctional protein ADE2 OS=Homo sapiens GN=PAICS PE=1 SV=3
212	Adenylate kinase isoenzyme 1 OS=Homo sapiens GN=AK1 PE=1 SV=3
213	SUMO-activating enzyme subunit 1 OS=Homo sapiens GN=SAE1 PE=1 SV=1
214	60S acidic ribosomal protein P1 OS=Homo sapiens GN=RPLP1 PE=1 SV=1
215	60S ribosomal protein L5 OS=Homo sapiens GN=RPL5 PE=1 SV=3
216	Caldesmon OS=Homo sapiens GN=CALD1 PE=1 SV=3
217	Thioredoxin domain-containing protein 17 OS=Homo sapiens GN=TXNDC17 PE=1 SV=1
218	Branched-chain-amino-acid aminotransferase, cytosolic OS=Homo sapiens GN=BCAT1 PE=1 SV=3
219	Reticulocalbin-1 OS=Homo sapiens GN=RCN1 PE=1 SV=1
220	V-type proton ATPase catalytic subunit A OS=Homo sapiens GN=ATP6V1A PE=1 SV=2
221	3-ketoacyl-CoA thiolase, mitochondrial OS=Homo sapiens GN=ACAA2 PE=1 SV=2
222	CTP synthase 1 OS=Homo sapiens GN=CTPS1 PE=1 SV=2
223	Ras suppressor protein 1 OS=Homo sapiens GN=RSU1 PE=1 SV=3
224	Fascin OS=Homo sapiens GN=FSCN1 PE=1 SV=3
225	Hsp90 co-chaperone Cdc37 OS=Homo sapiens GN=CDC37 PE=1 SV=1
226	Methionine adenosyltransferase 2 subunit beta OS=Homo sapiens GN=MAT2B PE=1 SV=1
227	Small nuclear ribonucleoprotein Sm D1 OS=Homo sapiens GN=SNRPD1 PE=1 SV=1
228	Peptidyl-prolyl cis-trans isomerase B OS=Homo sapiens GN=PPIB PE=1 SV=2
229	Peptidyl-prolyl cis-trans isomerase FKBP5 OS=Homo sapiens GN=FKBP5 PE=1 SV=2
230	Polyadenylate-binding protein 1 OS=Homo sapiens GN=PABPC1 PE=1 SV=2
231	5~(3~)-deoxyribonucleotidase, cytosolic type OS=Homo sapiens GN=NT5C PE=1 SV=2
232	Hyaluronan and proteoglycan link protein 1 OS=Homo sapiens GN=HAPLN1 PE=2 SV=2
233	ATP-dependent RNA helicase DDX39A OS=Homo sapiens GN=DDX39A PE=1 SV=2
234	Acetyl-CoA acetyltransferase, cytosolic OS=Homo sapiens GN=ACAT2 PE=1 SV=2
235	Acyl-CoA-binding protein OS=Homo sapiens GN=DBI PE=1 SV=2
236	Asparagine--tRNA ligase, cytoplasmic OS=Homo sapiens GN=NARS PE=1 SV=1
237	Eukaryotic translation initiation factor 4B OS=Homo sapiens GN=EIF4B PE=1 SV=2
238	Glutathione S-transferase Mu 2 OS=Homo sapiens GN=GSTM2 PE=1 SV=2
239	Adenylyl cyclase-associated protein 1 OS=Homo sapiens GN=CAP1 PE=1 SV=5
240	3-hydroxybutyrate dehydrogenase type 2 OS=Homo sapiens GN=BDH2 PE=1 SV=2
241	Carbonic anhydrase 2 OS=Homo sapiens GN=CA2 PE=1 SV=2
242	ATP-binding cassette sub-family E member 1 OS=Homo sapiens GN=ABCE1 PE=1 SV=1

243	Transgelin OS=Homo sapiens GN=TAGLN PE=1 SV=4
244	Eukaryotic translation initiation factor 5 OS=Homo sapiens GN=EIF5 PE=1 SV=2
245	Actin-related protein 3 OS=Homo sapiens GN=ACTR3 PE=1 SV=3
246	Myotrophin OS=Homo sapiens GN=MTPN PE=1 SV=2
247	Eukaryotic peptide chain release factor GTP-binding subunit ERF3A OS=Homo sapiens GN=GSPT1 PE=1 SV=1
248	Nuclear protein localization protein 4 homolog OS=Homo sapiens GN=NPLOC4 PE=1 SV=3
249	Cleavage and polyadenylation specificity factor subunit 6 OS=Homo sapiens GN=CPSF6 PE=1 SV=2
250	Putative cytochrome b-c1 complex subunit Rieske-like protein 1 OS=Homo sapiens GN=UQCRFS1P1 PE=5 SV=1
251	Serine--tRNA ligase, cytoplasmic OS=Homo sapiens GN=SARS PE=1 SV=3
252	Nuclear transport factor 2 OS=Homo sapiens GN=NUTF2 PE=1 SV=1
253	GMP synthase [glutamine-hydrolyzing] OS=Homo sapiens GN=GMPS PE=1 SV=1
254	Protein phosphatase methylesterase 1 OS=Homo sapiens GN=PPME1 PE=1 SV=3
255	Puromycin-sensitive aminopeptidase OS=Homo sapiens GN=NPEPPS PE=1 SV=2
256	Ran-specific GTPase-activating protein OS=Homo sapiens GN=RANBP1 PE=1 SV=1
257	Angio-associated migratory cell protein OS=Homo sapiens GN=AAMP PE=1 SV=2
258	Proteasome activator complex subunit 1 OS=Homo sapiens GN=PSME1 PE=1 SV=1
259	Bis(5~-nucleosyl)-tetraphosphatase [asymmetrical] OS=Homo sapiens GN=NUDT2 PE=1 SV=3
260	Peptidyl-prolyl cis-trans isomerase FKBP1A OS=Homo sapiens GN=FKBP1A PE=1 SV=2
261	Serine/threonine-protein phosphatase 2A 65 kDa regulatory subunit A alpha isoform OS=Homo sapiens GN=PPP2R1A PE=1 SV=4
262	Hematological and neurological expressed 1-like protein OS=Homo sapiens GN=HN1L PE=1 SV=1
263	Thioredoxin domain-containing protein 5 OS=Homo sapiens GN=TXNDC5 PE=1 SV=2
264	UV excision repair protein RAD23 homolog B OS=Homo sapiens GN=RAD23B PE=1 SV=1
265	N-acetylglucosamine-6-sulfatase OS=Homo sapiens GN=GNS PE=1 SV=3
266	Hepatoma-derived growth factor OS=Homo sapiens GN=HDGF PE=1 SV=1
267	Cytoplasmic aconitate hydratase OS=Homo sapiens GN=ACO1 PE=1 SV=3
268	Replication protein A 70 kDa DNA-binding subunit OS=Homo sapiens GN=RPA1 PE=1 SV=2
269	Gamma-glutamylcyclotransferase OS=Homo sapiens GN=GGCT PE=1 SV=1
270	Neuroblast differentiation-associated protein AHNAK OS=Homo sapiens GN=AHNAK PE=1 SV=2
271	Cyclin-dependent kinase 1 OS=Homo sapiens GN=CDK1 PE=1 SV=3
272	Ubiquitin carboxyl-terminal hydrolase 5 OS=Homo sapiens GN=USP5 PE=1 SV=2
273	Guanidinoacetate N-methyltransferase OS=Homo sapiens GN=GAMT PE=1 SV=1
274	3~(2~),5~-bisphosphate nucleotidase 1 OS=Homo sapiens GN=BPNT1 PE=1 SV=1
275	Nuclear migration protein nudC OS=Homo sapiens GN=NUDC PE=1 SV=1
276	Alpha-actinin-3 OS=Homo sapiens GN=ACTN3 PE=1 SV=2
277	Nardilysin OS=Homo sapiens GN=NRD1 PE=1 SV=2
278	High mobility group protein B1 OS=Homo sapiens GN=HMGB1 PE=1 SV=3
279	Pseudouridine-5~-phosphatase OS=Homo sapiens GN=HDHD1 PE=1 SV=3
280	Isopentenyl-diphosphate Delta-isomerase 1 OS=Homo sapiens GN=IDI1 PE=1 SV=2
281	Serine/threonine-protein phosphatase PP1-alpha catalytic subunit OS=Homo sapiens GN=PPP1CA PE=1 SV=1
282	Neurolysin, mitochondrial OS=Homo sapiens GN=NLN PE=1 SV=1
283	UMP-CMP kinase OS=Homo sapiens GN=CMPK1 PE=1 SV=3
284	Keratin, type II cytoskeletal 1 OS=Homo sapiens GN=KRT1 PE=1 SV=6
285	Eukaryotic translation initiation factor 6 OS=Homo sapiens GN=EIF6 PE=1 SV=1
286	Cytosolic purine 5~-nucleotidase OS=Homo sapiens GN=NT5C2 PE=1 SV=1
287	Sorting nexin-2 OS=Homo sapiens GN=SNX2 PE=1 SV=2

288	60S ribosomal protein L22 OS=Homo sapiens GN=RPL22 PE=1 SV=2
289	Peptidyl-prolyl cis-trans isomerase FKBP3 OS=Homo sapiens GN=FKBP3 PE=1 SV=1
290	Signal recognition particle 14 kDa protein OS=Homo sapiens GN=SRP14 PE=1 SV=2
291	Ubiquitin-40S ribosomal protein S27a OS=Homo sapiens GN=RPS27A PE=1 SV=2
292	Uridine 5~-monophosphate synthase OS=Homo sapiens GN=UMPS PE=1 SV=1
293	Programmed cell death protein 5 OS=Homo sapiens GN=PDCD5 PE=1 SV=3
294	tRNA (guanine-N(7)-)-methyltransferase OS=Homo sapiens GN=METTL1 PE=1 SV=1
295	Parathymosin OS=Homo sapiens GN=PTMS PE=1 SV=2
296	Histidine--tRNA ligase, cytoplasmic OS=Homo sapiens GN=HARS PE=1 SV=2
297	Delta-1-pyrroline-5-carboxylate synthase OS=Homo sapiens GN=ALDH18A1 PE=1 SV=2
298	Phosphoserine aminotransferase OS=Homo sapiens GN=PSAT1 PE=1 SV=2
299	Inosine triphosphate pyrophosphatase OS=Homo sapiens GN=ITPA PE=1 SV=2
300	Clathrin heavy chain 1 OS=Homo sapiens GN=CLTC PE=1 SV=5
301	Small ubiquitin-related modifier 2 OS=Homo sapiens GN=SUMO2 PE=1 SV=3
302	Dihydrolipoyl dehydrogenase, mitochondrial OS=Homo sapiens GN=DLD PE=1 SV=2
303	Ribonuclease inhibitor OS=Homo sapiens GN=RNH1 PE=1 SV=2
304	Protein C10 OS=Homo sapiens GN=C12orf57 PE=1 SV=1
305	Phospholipase D3 OS=Homo sapiens GN=PLD3 PE=1 SV=1
306	Hydroxyacyl-coenzyme A dehydrogenase, mitochondrial OS=Homo sapiens GN=HADH PE=1 SV=3
307	Heterogeneous nuclear ribonucleoprotein F OS=Homo sapiens GN=HNRNPF PE=1 SV=3
308	Histone-binding protein RBBP4 OS=Homo sapiens GN=RBBP4 PE=1 SV=3
309	Ovarian cancer-associated gene 2 protein OS=Homo sapiens GN=OVCA2 PE=1 SV=1
310	Farnesyl pyrophosphate synthase OS=Homo sapiens GN=FDPS PE=1 SV=4
311	UDP-N-acetylhexosamine pyrophosphorylase OS=Homo sapiens GN=UAP1 PE=1 SV=3
312	Alpha-N-acetylgalactosaminidase OS=Homo sapiens GN=NAGA PE=1 SV=2
313	Ubiquitin thioesterase OTUB1 OS=Homo sapiens GN=OTUB1 PE=1 SV=2
314	Importin subunit alpha-1 OS=Homo sapiens GN=KPNA2 PE=1 SV=1
315	ERO1-like protein alpha OS=Homo sapiens GN=ERO1A PE=1 SV=2
316	Secernin-1 OS=Homo sapiens GN=SCRN1 PE=1 SV=2
317	Serine hydroxymethyltransferase, cytosolic OS=Homo sapiens GN=SHMT1 PE=1 SV=1
318	Myosin-9 OS=Homo sapiens GN=MYH9 PE=1 SV=4
319	Zyxin OS=Homo sapiens GN=ZYX PE=1 SV=1
320	Pirin OS=Homo sapiens GN=PIR PE=1 SV=1
321	Heterogeneous nuclear ribonucleoprotein A1-like 2 OS=Homo sapiens GN=HNRNPA1L2 PE=2 SV=2
322	Prefoldin subunit 4 OS=Homo sapiens GN=PFDN4 PE=1 SV=1
323	Myeloid-derived growth factor OS=Homo sapiens GN=MYDGF PE=1 SV=1
324	Sialic acid synthase OS=Homo sapiens GN=NANS PE=1 SV=2
325	Ribosomal protein S6 kinase alpha-3 OS=Homo sapiens GN=RPS6KA3 PE=1 SV=1
326	Stathmin OS=Homo sapiens GN=STMN1 PE=1 SV=3
327	Platelet-activating factor acetylhydrolase IB subunit gamma OS=Homo sapiens GN=PAFAH1B3 PE=1 SV=1
328	Enolase-phosphatase E1 OS=Homo sapiens GN=ENOPH1 PE=1 SV=1
329	Elongation factor 1-gamma OS=Homo sapiens GN=EEF1G PE=1 SV=3
330	SH3 domain-binding glutamic acid-rich-like protein 3 OS=Homo sapiens GN=SH3BGRL3 PE=1 SV=1
331	Methylosome subunit pICln OS=Homo sapiens GN=CLNS1A PE=1 SV=1
332	Hematological and neurological expressed 1 protein OS=Homo sapiens GN=HN1 PE=1 SV=3
333	Nicotinamide phosphoribosyltransferase OS=Homo sapiens GN=NAMPT PE=1 SV=1
334	Protein phosphatase 1 regulatory subunit 12A OS=Homo sapiens GN=PPP1R12A PE=1 SV=1

335	ADP-ribosylation factor 1 OS=Homo sapiens GN=ARF1 PE=1 SV=2
336	T-complex protein 1 subunit theta OS=Homo sapiens GN=CCT8 PE=1 SV=4
337	Glutathione S-transferase Mu 1 OS=Homo sapiens GN=GSTM1 PE=1 SV=3
338	Thioredoxin-like protein 1 OS=Homo sapiens GN=TXNL1 PE=1 SV=3
339	T-complex protein 1 subunit epsilon OS=Homo sapiens GN=CCT5 PE=1 SV=1
340	F-actin-capping protein subunit beta OS=Homo sapiens GN=CAPZB PE=1 SV=4
341	Adenylate kinase 2, mitochondrial OS=Homo sapiens GN=AK2 PE=1 SV=2
342	Intraflagellar transport protein 25 homolog OS=Homo sapiens GN=HSPB11 PE=1 SV=1
343	UPF0489 protein C5orf22 OS=Homo sapiens GN=C5orf22 PE=1 SV=2
344	NAD(P)H-hydrate epimerase OS=Homo sapiens GN=APOA1BP PE=1 SV=2
345	Adenylate kinase isoenzyme 6 OS=Homo sapiens GN=AK6 PE=1 SV=1
346	Lamina-associated polypeptide 2, isoform alpha OS=Homo sapiens GN=TMPO PE=1 SV=2
347	Heme-binding protein 1 OS=Homo sapiens GN=HEBP1 PE=1 SV=1
348	Protein S100-A4 OS=Homo sapiens GN=S100A4 PE=1 SV=1
349	HCLS1-binding protein 3 OS=Homo sapiens GN=HS1BP3 PE=1 SV=1
350	Ubiquitin-fold modifier 1 OS=Homo sapiens GN=UFM1 PE=1 SV=1
351	Prefoldin subunit 2 OS=Homo sapiens GN=PFDN2 PE=1 SV=1
352	Proliferation-associated protein 2G4 OS=Homo sapiens GN=PA2G4 PE=1 SV=3
353	Kinectin OS=Homo sapiens GN=KTN1 PE=1 SV=1
354	Serine/arginine-rich splicing factor 2 OS=Homo sapiens GN=SRSF2 PE=1 SV=4
355	Ubiquitin-conjugating enzyme E2 N OS=Homo sapiens GN=UBE2N PE=1 SV=1
356	Developmentally-regulated GTP-binding protein 1 OS=Homo sapiens GN=DRG1 PE=1 SV=1
357	Poly(rC)-binding protein 2 OS=Homo sapiens GN=PCBP2 PE=1 SV=1
358	Histidine triad nucleotide-binding protein 2, mitochondrial OS=Homo sapiens GN=HINT2 PE=1 SV=1
359	Ribonucleoside-diphosphate reductase large subunit OS=Homo sapiens GN=RRM1 PE=1 SV=1
360	Oxysterol-binding protein 1 OS=Homo sapiens GN=OSBP PE=1 SV=1
361	Translin OS=Homo sapiens GN=TSN PE=1 SV=1
362	Calcyclin-binding protein OS=Homo sapiens GN=CACYBP PE=1 SV=2
363	SH3 domain-binding glutamic acid-rich protein OS=Homo sapiens GN=SH3BGR PE=2 SV=3
364	7,8-dihydro-8-oxoguanine triphosphatase OS=Homo sapiens GN=NUDT1 PE=1 SV=3
365	40S ribosomal protein S21 OS=Homo sapiens GN=RPS21 PE=1 SV=1
366	Flap endonuclease 1 OS=Homo sapiens GN=FEN1 PE=1 SV=1
367	Adenylosuccinate synthetase isozyme 2 OS=Homo sapiens GN=ADSS PE=1 SV=3
368	Inositol-3-phosphate synthase 1 OS=Homo sapiens GN=ISYNA1 PE=1 SV=1
369	Septin-2 OS=Homo sapiens GN=SEPT2 PE=1 SV=1
370	Spectrin alpha chain, non-erythrocytic 1 OS=Homo sapiens GN=SPTAN1 PE=1 SV=3
371	Histone acetyltransferase type B catalytic subunit OS=Homo sapiens GN=HAT1 PE=1 SV=1
372	Deoxyhypusine hydroxylase OS=Homo sapiens GN=DOHH PE=1 SV=1
373	Prostaglandin reductase 2 OS=Homo sapiens GN=PTGR2 PE=1 SV=1
374	Splicing factor 1 OS=Homo sapiens GN=SF1 PE=1 SV=4
375	NAD(P)H dehydrogenase [quinone] 1 OS=Homo sapiens GN=NQO1 PE=1 SV=1
376	Serine/threonine-protein phosphatase 2A 55 kDa regulatory subunit B alpha isoform OS=Homo sapiens GN=PPP2R2A PE=1 SV=1
377	Proteasome subunit beta type-1 OS=Homo sapiens GN=PSMB1 PE=1 SV=2
378	Asparagine synthetase [glutamine-hydrolyzing] OS=Homo sapiens GN=ASNS PE=1 SV=4
379	Cellular retinoic acid-binding protein 2 OS=Homo sapiens GN=CRABP2 PE=1 SV=2
380	ATP-citrate synthase OS=Homo sapiens GN=ACLY PE=1 SV=3
381	Serine/threonine-protein kinase OSR1 OS=Homo sapiens GN=OXSR1 PE=1 SV=1

382	S-phase kinase-associated protein 1 OS=Homo sapiens GN=SKP1 PE=1 SV=2
383	C-1-tetrahydrofolate synthase, cytoplasmic OS=Homo sapiens GN=MTHFD1 PE=1 SV=3
384	Interleukin enhancer-binding factor 2 OS=Homo sapiens GN=ILF2 PE=1 SV=2
385	Transforming protein RhoA OS=Homo sapiens GN=RHOA PE=1 SV=1
386	Transcription intermediary factor 1-beta OS=Homo sapiens GN=TRIM28 PE=1 SV=5
387	Transcription elongation factor B polypeptide 1 OS=Homo sapiens GN=TCEB1 PE=1 SV=1
388	Ubiquitin-like modifier-activating enzyme 6 OS=Homo sapiens GN=UBA6 PE=1 SV=1
389	Zinc finger MYM-type protein 3 OS=Homo sapiens GN=ZMYM3 PE=1 SV=2
390	T-complex protein 1 subunit delta OS=Homo sapiens GN=CCT4 PE=1 SV=4
391	Elongation factor Tu, mitochondrial OS=Homo sapiens GN=TUFM PE=1 SV=2
392	Uroporphyrinogen decarboxylase OS=Homo sapiens GN=UROD PE=1 SV=2
393	WD repeat-containing protein 1 OS=Homo sapiens GN=WDR1 PE=1 SV=4
394	Fatty acid synthase OS=Homo sapiens GN=FASN PE=1 SV=3
395	Inositol monophosphatase 1 OS=Homo sapiens GN=IMPA1 PE=1 SV=1
396	Deoxyhypusine synthase OS=Homo sapiens GN=DHPS PE=1 SV=1
397	Vigilin OS=Homo sapiens GN=HDLBP PE=1 SV=2
398	Citrate synthase, mitochondrial OS=Homo sapiens GN=CS PE=1 SV=2
399	40S ribosomal protein S28 OS=Homo sapiens GN=RPS28 PE=1 SV=1
400	Rho GDP-dissociation inhibitor 1 OS=Homo sapiens GN=ARHGDIA PE=1 SV=3
401	Phosphatidylinositol-binding clathrin assembly protein OS=Homo sapiens GN=PICALM PE=1 SV=2
402	Activator of 90 kDa heat shock protein ATPase homolog 1 OS=Homo sapiens GN=AHSA1 PE=1 SV=1
403	Mitochondrial import receptor subunit TOM34 OS=Homo sapiens GN=TOMM34 PE=1 SV=2
404	Eukaryotic translation initiation factor 3 subunit F OS=Homo sapiens GN=EIF3F PE=1 SV=1
405	Threonine--tRNA ligase, cytoplasmic OS=Homo sapiens GN=TARS PE=1 SV=3
406	Importin-7 OS=Homo sapiens GN=IPO7 PE=1 SV=1
407	26S protease regulatory subunit 6A OS=Homo sapiens GN=PSMC3 PE=1 SV=3
408	Charged multivesicular body protein 4b OS=Homo sapiens GN=CHMP4B PE=1 SV=1
409	LIM and SH3 domain protein 1 OS=Homo sapiens GN=LASP1 PE=1 SV=2
410	DNA fragmentation factor subunit alpha OS=Homo sapiens GN=DFFA PE=1 SV=1
411	Glucose-6-phosphate 1-dehydrogenase OS=Homo sapiens GN=G6PD PE=1 SV=4
412	Lon protease homolog, mitochondrial OS=Homo sapiens GN=LONP1 PE=1 SV=2
413	Nuclease-sensitive element-binding protein 1 OS=Homo sapiens GN=YBX1 PE=1 SV=3
414	Profilin-2 OS=Homo sapiens GN=PFN2 PE=1 SV=3
415	Nucleolysin TIA-1 isoform p40 OS=Homo sapiens GN=TIA1 PE=1 SV=3
416	Far upstream element-binding protein 2 OS=Homo sapiens GN=KHSRP PE=1 SV=4
417	Quinone oxidoreductase OS=Homo sapiens GN=CRYZ PE=1 SV=1
418	Thioredoxin domain-containing protein 12 OS=Homo sapiens GN=TXNDC12 PE=1 SV=1
419	Spermidine synthase OS=Homo sapiens GN=SRM PE=1 SV=1
420	Aspartate aminotransferase, mitochondrial OS=Homo sapiens GN=GOT2 PE=1 SV=3
421	Splicing factor 3A subunit 3 OS=Homo sapiens GN=SF3A3 PE=1 SV=1
422	Heterogeneous nuclear ribonucleoprotein U OS=Homo sapiens GN=HNRNPU PE=1 SV=6
423	FAS-associated factor 1 OS=Homo sapiens GN=FAF1 PE=1 SV=2
424	Alpha-centractin OS=Homo sapiens GN=ACTR1A PE=1 SV=1
425	L-aminoadipate-semialdehyde dehydrogenase-phosphopantetheinyl transferase OS=Homo sapiens GN=AASDHPPT PE=1 SV=2
426	Tyrosine--tRNA ligase, mitochondrial OS=Homo sapiens GN=YARS2 PE=1 SV=2
427	DNA damage-binding protein 1 OS=Homo sapiens GN=DDB1 PE=1 SV=1
428	Serpin B6 OS=Homo sapiens GN=SERPINB6 PE=1 SV=3

429	NSFL1 cofactor p47 OS=Homo sapiens GN=NSFL1C PE=1 SV=2
430	SUMO-conjugating enzyme UBC9 OS=Homo sapiens GN=UBE2I PE=1 SV=1
431	Eukaryotic translation initiation factor 5A-1 OS=Homo sapiens GN=EIF5A PE=1 SV=2
432	ADP-ribosylation factor-like protein 3 OS=Homo sapiens GN=ARL3 PE=1 SV=2
433	Low molecular weight phosphotyrosine protein phosphatase OS=Homo sapiens GN=ACP1 PE=1 SV=3
434	Target of Myb protein 1 OS=Homo sapiens GN=TOM1 PE=1 SV=2
435	Translation machinery-associated protein 7 OS=Homo sapiens GN=TMA7 PE=1 SV=1
436	Astrocytic phosphoprotein PEA-15 OS=Homo sapiens GN=PEA15 PE=1 SV=2
437	DNA ligase 1 OS=Homo sapiens GN=LIG1 PE=1 SV=1
438	Mothers against decapentaplegic homolog 4 OS=Homo sapiens GN=SMAD4 PE=1 SV=1
439	Prefoldin subunit 6 OS=Homo sapiens GN=PFDN6 PE=1 SV=1
440	ATP-dependent 6-phosphofructokinase, muscle type OS=Homo sapiens GN=PFKM PE=1 SV=2
441	Serine/threonine-protein phosphatase 2A catalytic subunit alpha isoform OS=Homo sapiens GN=PPP2CA PE=1 SV=1
442	UPF0600 protein C5orf51 OS=Homo sapiens GN=C5orf51 PE=1 SV=1
443	Protein transport protein Sec31A OS=Homo sapiens GN=SEC31A PE=1 SV=3
444	Eukaryotic translation initiation factor 2 subunit 1 OS=Homo sapiens GN=EIF2S1 PE=1 SV=3
445	Mitochondrial-processing peptidase subunit alpha OS=Homo sapiens GN=PMPCA PE=1 SV=2
446	Transcription factor BTF3 homolog 4 OS=Homo sapiens GN=BTF3L4 PE=1 SV=1
447	Nuclear ubiquitous casein and cyclin-dependent kinase substrate 1 OS=Homo sapiens GN=NUCKS1 PE=1 SV=1
448	Protein SGT1 homolog OS=Homo sapiens GN=SUGT1 PE=1 SV=3
449	Deoxyuridine 5~-triphosphate nucleotidohydrolase, mitochondrial OS=Homo sapiens GN=DUT PE=1 SV=4
450	GrpE protein homolog 1, mitochondrial OS=Homo sapiens GN=GRPEL1 PE=1 SV=2
451	Myc box-dependent-interacting protein 1 OS=Homo sapiens GN=BIN1 PE=1 SV=1
452	Calumenin OS=Homo sapiens GN=CALU PE=1 SV=2
453	Prolyl 3-hydroxylase OGFOD1 OS=Homo sapiens GN=OGFOD1 PE=1 SV=1
454	Glia maturation factor beta OS=Homo sapiens GN=GMFB PE=1 SV=2
455	Copine-1 OS=Homo sapiens GN=CPNE1 PE=1 SV=1
456	Heterogeneous nuclear ribonucleoprotein D0 OS=Homo sapiens GN=HNRNPD PE=1 SV=1
457	Serpin B9 OS=Homo sapiens GN=SERPINB9 PE=1 SV=1
458	Acyl-protein thioesterase 1 OS=Homo sapiens GN=LYPLA1 PE=1 SV=1
459	Transcription elongation factor A protein 1 OS=Homo sapiens GN=TCEA1 PE=1 SV=2
460	Protein archease OS=Homo sapiens GN=ZBTB8OS PE=1 SV=2
461	Rap1 GTPase-GDP dissociation stimulator 1 OS=Homo sapiens GN=RAP1GDS1 PE=1 SV=3
462	Inositol hexakisphosphate and diphosphoinositol-pentakisphosphate kinase 1 OS=Homo sapiens GN=PPIP5K1 PE=1 SV=1
463	Ataxin-10 OS=Homo sapiens GN=ATXN10 PE=1 SV=1
464	NADPH:adrenodoxin oxidoreductase, mitochondrial OS=Homo sapiens GN=FDXR PE=1 SV=3
465	Copine-2 OS=Homo sapiens GN=CPNE2 PE=1 SV=3
466	Creatine kinase B-type OS=Homo sapiens GN=CKB PE=1 SV=1
467	Putative FK506-binding protein 9-like protein OS=Homo sapiens GN=FKBP9P1 PE=5 SV=1
468	Actin-related protein 2/3 complex subunit 4 OS=Homo sapiens GN=ARPC4 PE=1 SV=3
469	Cullin-associated NEDD8-dissociated protein 1 OS=Homo sapiens GN=CAND1 PE=1 SV=2
470	Insulin-degrading enzyme OS=Homo sapiens GN=IDE PE=1 SV=4
471	Ubiquitin carboxyl-terminal hydrolase isozyme L1 OS=Homo sapiens GN=UCHL1 PE=1 SV=2
472	Protein CutA OS=Homo sapiens GN=CUTA PE=1 SV=2

473	Aldo-keto reductase family 1 member C1 OS=Homo sapiens GN=AKR1C1 PE=1 SV=1
474	60S ribosomal protein L11 OS=Homo sapiens GN=RPL11 PE=1 SV=2
475	Heterogeneous nuclear ribonucleoprotein A/B OS=Homo sapiens GN=HNRNPAB PE=1 SV=2
476	Tight junction protein ZO-1 OS=Homo sapiens GN=TJP1 PE=1 SV=3
477	Fumarate hydratase, mitochondrial OS=Homo sapiens GN=FH PE=1 SV=3
478	Beta-hexosaminidase subunit alpha OS=Homo sapiens GN=HEXA PE=1 SV=2
479	dCTP pyrophosphatase 1 OS=Homo sapiens GN=DCTPP1 PE=1 SV=1
480	Vasodilator-stimulated phosphoprotein OS=Homo sapiens GN=VASP PE=1 SV=3
481	Eukaryotic translation initiation factor 4 gamma 2 OS=Homo sapiens GN=EIF4G2 PE=1 SV=1
482	Fidgetin-like protein 1 OS=Homo sapiens GN=FIGNL1 PE=1 SV=2
483	UDP-glucose:glycoprotein glucosyltransferase 1 OS=Homo sapiens GN=UGGT1 PE=1 SV=3
484	U8 snoRNA-decapping enzyme OS=Homo sapiens GN=NUDT16 PE=1 SV=2
485	Poly(U)-binding-splicing factor PUF60 OS=Homo sapiens GN=PUF60 PE=1 SV=1
486	Multiple inositol polyphosphate phosphatase 1 OS=Homo sapiens GN=MINPP1 PE=1 SV=1
487	Ubiquitin-conjugating enzyme E2 variant 1 OS=Homo sapiens GN=UBE2V1 PE=1 SV=2
488	Transcription elongation factor B polypeptide 2 OS=Homo sapiens GN=TCEB2 PE=1 SV=1
489	Ubiquitin-associated protein 2-like OS=Homo sapiens GN=UBAP2L PE=1 SV=2
490	Ras GTPase-activating-like protein IQGAP1 OS=Homo sapiens GN=IQGAP1 PE=1 SV=1
491	Cytosolic acyl coenzyme A thioester hydrolase OS=Homo sapiens GN=ACOT7 PE=1 SV=3
492	Protocadherin Fat 3 OS=Homo sapiens GN=FAT3 PE=2 SV=2
493	Protein PBDC1 OS=Homo sapiens GN=PBDC1 PE=1 SV=1
494	Alpha-endosulfine OS=Homo sapiens GN=ENSA PE=1 SV=1
495	Ubiquitin thioesterase OTUB2 OS=Homo sapiens GN=OTUB2 PE=1 SV=2
496	Ribonucleoside-diphosphate reductase subunit M2 B OS=Homo sapiens GN=RRM2B PE=1 SV=1
497	Developmentally-regulated GTP-binding protein 2 OS=Homo sapiens GN=DRG2 PE=1 SV=1
498	6-phosphogluconolactonase OS=Homo sapiens GN=PGLS PE=1 SV=2
499	Cytoplasmic dynein 1 light intermediate chain 1 OS=Homo sapiens GN=DYNC1LI1 PE=1 SV=3

Table S4 Identified protein list for A2780 cell lysate. The protein with the highest protein score is hit number 1 and so on.

	SiNPs - A2780 cell lysate
1	Nucleolin OS=Homo sapiens GN=NCL PE=1 SV=3
2	Histone H2B type 1-C/E/F/G/I OS=Homo sapiens GN=HIST1H2BC PE=1 SV=4
3	Keratin, type II cytoskeletal 1 OS=Homo sapiens GN=KRT1 PE=1 SV=6
4	Keratin, type I cytoskeletal 9 OS=Homo sapiens GN=KRT9 PE=1 SV=3
5	Histone H1.2 OS=Homo sapiens GN=HIST1H1C PE=1 SV=2
6	Ribosome-binding protein 1 OS=Homo sapiens GN=RRBP1 PE=1 SV=4
7	Histone H2A type 1-D OS=Homo sapiens GN=HIST1H2AD PE=1 SV=2
8	10 kDa heat shock protein, mitochondrial OS=Homo sapiens GN=HSPE1 PE=1 SV=2
9	Malate dehydrogenase, mitochondrial OS=Homo sapiens GN=MDH2 PE=1 SV=3
10	Keratin, type I cytoskeletal 10 OS=Homo sapiens GN=KRT10 PE=1 SV=6
11	Heterogeneous nuclear ribonucleoprotein K OS=Homo sapiens GN=HNRNPK PE=1 SV=1
12	Heterogeneous nuclear ribonucleoprotein U OS=Homo sapiens GN=HNRNPU PE=1 SV=6
13	Actin, cytoplasmic 1 OS=Homo sapiens GN=ACTB PE=1 SV=1
14	Histone H4 OS=Homo sapiens GN=HIST1H4A PE=1 SV=2

15	Nucleophosmin OS=Homo sapiens GN=NPM1 PE=1 SV=2
16	60S ribosomal protein L14 OS=Homo sapiens GN=RPL14 PE=1 SV=4
17	Aspartate aminotransferase, mitochondrial OS=Homo sapiens GN=GOT2 PE=1 SV=3
18	Heterogeneous nuclear ribonucleoprotein A1 OS=Homo sapiens GN=HNRNPA1 PE=1 SV=5
19	Heterogeneous nuclear ribonucleoproteins A2/B1 OS=Homo sapiens GN=HNRNPA2B1 PE=1 SV=2
20	Splicing factor, proline- and glutamine-rich OS=Homo sapiens GN=SFPQ PE=1 SV=2
21	Elongation factor 1-alpha 1 OS=Homo sapiens GN=EEF1A1 PE=1 SV=1
22	Tubulin alpha-1B chain OS=Homo sapiens GN=TUBA1B PE=1 SV=1
23	Heterogeneous nuclear ribonucleoprotein A0 OS=Homo sapiens GN=HNRNPA0 PE=1 SV=1
24	Heterogeneous nuclear ribonucleoprotein A3 OS=Homo sapiens GN=HNRNPA3 PE=1 SV=2
25	RNA-binding motif protein, X chromosome OS=Homo sapiens GN=RBMX PE=1 SV=3
26	Alpha-enolase OS=Homo sapiens GN=ENO1 PE=1 SV=2
27	Peroxiredoxin-1 OS=Homo sapiens GN=PRDX1 PE=1 SV=1
28	40S ribosomal protein S8 OS=Homo sapiens GN=RPS8 PE=1 SV=2
29	Spectrin beta chain, non-erythrocytic 1 OS=Homo sapiens GN=SPTBN1 PE=1 SV=2
30	Dermcidin OS=Homo sapiens GN=DCD PE=1 SV=2
31	Polyadenylate-binding protein 1 OS=Homo sapiens GN=PABPC1 PE=1 SV=2
32	Heterogeneous nuclear ribonucleoprotein R OS=Homo sapiens GN=HNRNPR PE=1 SV=1
33	Cytoskeleton-associated protein 4 OS=Homo sapiens GN=CKAP4 PE=1 SV=2
34	60 kDa heat shock protein, mitochondrial OS=Homo sapiens GN=HSPD1 PE=1 SV=2
35	RNA-binding protein FUS OS=Homo sapiens GN=FUS PE=1 SV=1
36	Heterogeneous nuclear ribonucleoprotein L OS=Homo sapiens GN=HNRNPL PE=1 SV=2
37	Plasminogen activator inhibitor 1 RNA-binding protein OS=Homo sapiens GN=SERBP1 PE=1 SV=2
38	Histone H3.1t OS=Homo sapiens GN=HIST3H3 PE=1 SV=3
39	Non-POU domain-containing octamer-binding protein OS=Homo sapiens GN=NONO PE=1 SV=4
40	Small nuclear ribonucleoprotein Sm D1 OS=Homo sapiens GN=SNRPD1 PE=1 SV=1
41	Glyceraldehyde-3-phosphate dehydrogenase OS=Homo sapiens GN=GAPDH PE=1 SV=3
42	60S ribosomal protein L23a OS=Homo sapiens GN=RPL23A PE=1 SV=1
43	Probable ATP-dependent RNA helicase DDX17 OS=Homo sapiens GN=DDX17 PE=1 SV=2
44	Far upstream element-binding protein 2 OS=Homo sapiens GN=KHSRP PE=1 SV=4
45	60S ribosomal protein L4 OS=Homo sapiens GN=RPL4 PE=1 SV=5
46	60S ribosomal protein L13 OS=Homo sapiens GN=RPL13 PE=1 SV=4
47	40S ribosomal protein S25 OS=Homo sapiens GN=RPS25 PE=1 SV=1
48	Paraspeckle component 1 OS=Homo sapiens GN=PSPC1 PE=1 SV=1
49	Cleavage and polyadenylation specificity factor subunit 6 OS=Homo sapiens GN=CPSF6 PE=1 SV=2
50	Glucose-6-phosphate isomerase OS=Homo sapiens GN=GPI PE=1 SV=4
51	Small nuclear ribonucleoprotein-associated proteins B and B~ OS=Homo sapiens GN=SNRPB PE=1 SV=2
52	Putative ribosomal RNA methyltransferase NOP2 OS=Homo sapiens GN=NOP2 PE=1 SV=2
53	Heterogeneous nuclear ribonucleoprotein D-like OS=Homo sapiens GN=HNRNPDL PE=1 SV=3
54	Nucleolar RNA helicase 2 OS=Homo sapiens GN=DDX21 PE=1 SV=5
55	Leucine-rich repeat-containing protein 59 OS=Homo sapiens GN=LRRC59 PE=1 SV=1
56	60S ribosomal protein L6 OS=Homo sapiens GN=RPL6 PE=1 SV=3
57	Heterogeneous nuclear ribonucleoprotein F OS=Homo sapiens GN=HNRNPF PE=1 SV=3
58	Far upstream element-binding protein 1 OS=Homo sapiens GN=FUBP1 PE=1 SV=3
59	60S ribosomal protein L7a OS=Homo sapiens GN=RPL7A PE=1 SV=2
60	60S ribosomal protein L18 OS=Homo sapiens GN=RPL18 PE=1 SV=2
61	40S ribosomal protein S26 OS=Homo sapiens GN=RPS26 PE=1 SV=3

62	Cleavage and polyadenylation specificity factor subunit 7 OS=Homo sapiens GN=CPSF7 PE=1 SV=1
63	Ribosomal L1 domain-containing protein 1 OS=Homo sapiens GN=RSL1D1 PE=1 SV=3
64	Adenylyl cyclase-associated protein 1 OS=Homo sapiens GN=CAP1 PE=1 SV=5
65	60S ribosomal protein L24 OS=Homo sapiens GN=RPL24 PE=1 SV=1
66	Filamin-A OS=Homo sapiens GN=FLNA PE=1 SV=4
67	Nucleoside diphosphate kinase A OS=Homo sapiens GN=NME1 PE=1 SV=1
68	DAZ-associated protein 1 OS=Homo sapiens GN=DAZAP1 PE=1 SV=1
69	Profilin-1 OS=Homo sapiens GN=PFN1 PE=1 SV=2
70	40S ribosomal protein S2 OS=Homo sapiens GN=RPS2 PE=1 SV=2
71	RNA-binding protein 39 OS=Homo sapiens GN=RBM39 PE=1 SV=2
72	Tubulin beta chain OS=Homo sapiens GN=TUBB PE=1 SV=2
73	Serpin H1 OS=Homo sapiens GN=SERPINH1 PE=1 SV=2
74	Histone H1.0 OS=Homo sapiens GN=H1F0 PE=1 SV=3
75	Fibronectin OS=Homo sapiens GN=FN1 PE=1 SV=4
76	60S ribosomal protein L8 OS=Homo sapiens GN=RPL8 PE=1 SV=2
77	Calreticulin OS=Homo sapiens GN=CALR PE=1 SV=1
78	H/ACA ribonucleoprotein complex subunit 4 OS=Homo sapiens GN=DKC1 PE=1 SV=3
79	Serine/arginine-rich splicing factor 10 OS=Homo sapiens GN=SRSF10 PE=1 SV=1
80	60S ribosomal protein L19 OS=Homo sapiens GN=RPL19 PE=1 SV=1
81	rRNA 2~-O-methyltransferase fibrillarin OS=Homo sapiens GN=FBL PE=1 SV=2
82	40S ribosomal protein S10 OS=Homo sapiens GN=RPS10 PE=1 SV=1
83	Centromere protein V OS=Homo sapiens GN=CENPV PE=1 SV=1
84	Chromobox protein homolog 3 OS=Homo sapiens GN=CBX3 PE=1 SV=4
85	Calcium-regulated heat stable protein 1 OS=Homo sapiens GN=CARHSP1 PE=1 SV=2
86	Small nuclear ribonucleoprotein Sm D2 OS=Homo sapiens GN=SNRPD2 PE=1 SV=1
87	Superoxide dismutase [Mn], mitochondrial OS=Homo sapiens GN=SOD2 PE=1 SV=2
88	Heterogeneous nuclear ribonucleoprotein C-like 1 OS=Homo sapiens GN=HNRNPCL1 PE=1 SV=1
89	Polypeptide N-acetylgalactosaminyltransferase 13 OS=Homo sapiens GN=GALNT13 PE=2 SV=2
90	Wolframin OS=Homo sapiens GN=WFS1 PE=1 SV=2
91	Long-chain-fatty-acid--CoA ligase 4 OS=Homo sapiens GN=ACSL4 PE=1 SV=2
92	Serine/arginine-rich splicing factor 11 OS=Homo sapiens GN=SRSF11 PE=1 SV=1
93	LIM and SH3 domain protein 1 OS=Homo sapiens GN=LASP1 PE=1 SV=2
94	DNA-(apurinic or apyrimidinic site) lyase OS=Homo sapiens GN=APEX1 PE=1 SV=2
95	RNA-binding protein EWS OS=Homo sapiens GN=EWSR1 PE=1 SV=1
96	Phosphatidylethanolamine-binding protein 1 OS=Homo sapiens GN=PEBP1 PE=1 SV=3
97	60S ribosomal protein L15 OS=Homo sapiens GN=RPL15 PE=1 SV=2
98	Histone H1.5 OS=Homo sapiens GN=HIST1H1B PE=1 SV=3
99	Activated RNA polymerase II transcriptional coactivator p15 OS=Homo sapiens GN=SUB1 PE=1 SV=3
100	Glutathione reductase, mitochondrial OS=Homo sapiens GN=GSR PE=1 SV=2
101	Golgi reassembly-stacking protein 2 OS=Homo sapiens GN=GORASP2 PE=1 SV=3
102	Peptidyl-prolyl cis-trans isomerase A OS=Homo sapiens GN=PPIA PE=1 SV=2
103	Ubiquinone biosynthesis monooxygenase COQ6 OS=Homo sapiens GN=COQ6 PE=1 SV=2
104	Nucleolar and coiled-body phosphoprotein 1 OS=Homo sapiens GN=NOLC1 PE=1 SV=2
105	Echinoderm microtubule-associated protein-like 4 OS=Homo sapiens GN=EML4 PE=1 SV=3
106	60S ribosomal protein L29 OS=Homo sapiens GN=RPL29 PE=1 SV=2
107	Core histone macro-H2A.1 OS=Homo sapiens GN=H2AFY PE=1 SV=4
108	40S ribosomal protein S28 OS=Homo sapiens GN=RPS28 PE=1 SV=1
109	Thioredoxin-dependent peroxide reductase, mitochondrial OS=Homo sapiens GN=PRDX3 PE=1 SV=3

Table S5 Identified protein list from the protein corona of SiNPs exposed to A2780 cell lysate. The protein with the highest protein score is hit number 1 and so on.

	AuNPs - A2780 cell lysate
1	Keratin, type II cytoskeletal 1 OS=Homo sapiens GN=KRT1 PE=1 SV=6
2	Keratin, type I cytoskeletal 10 OS=Homo sapiens GN=KRT10 PE=1 SV=6
3	Dermcidin OS=Homo sapiens GN=DCD PE=1 SV=2
4	Alpha-enolase OS=Homo sapiens GN=ENO1 PE=1 SV=2
5	Actin, cytoplasmic 1 OS=Homo sapiens GN=ACTB PE=1 SV=1
6	Histone H1.2 OS=Homo sapiens GN=HIST1H1C PE=1 SV=2
7	60S ribosomal protein L14 OS=Homo sapiens GN=RPL14 PE=1 SV=4
8	Ribosome-binding protein 1 OS=Homo sapiens GN=RRBP1 PE=1 SV=4
9	Splicing factor, proline- and glutamine-rich OS=Homo sapiens GN=SFPQ PE=1 SV=2
10	Tubulin alpha-1A chain OS=Homo sapiens GN=TUBA1A PE=1 SV=1
11	Catalase OS=Homo sapiens GN=CAT PE=1 SV=3
12	Histone H4 OS=Homo sapiens GN=HIST1H4A PE=1 SV=2
13	10 kDa heat shock protein, mitochondrial OS=Homo sapiens GN=HSPE1 PE=1 SV=2
14	Filaggrin-2 OS=Homo sapiens GN=FLG2 PE=1 SV=1
15	Desmoplakin OS=Homo sapiens GN=DSP PE=1 SV=3
16	Filamin-A OS=Homo sapiens GN=FLNA PE=1 SV=4
17	Small proline-rich protein 2D OS=Homo sapiens GN=SPRR2D PE=2 SV=2
18	Putative zinc-alpha-2-glycoprotein-like 1 OS=Homo sapiens PE=5 SV=2
19	Hornerin OS=Homo sapiens GN=HRNR PE=1 SV=2
20	Cathepsin B OS=Homo sapiens GN=CTSB PE=1 SV=3
21	Retrotransposon-derived protein PEG10 OS=Homo sapiens GN=PEG10 PE=1 SV=2
22	Histone H3.3C OS=Homo sapiens GN=H3F3C PE=1 SV=3
23	60 kDa heat shock protein, mitochondrial OS=Homo sapiens GN=HSPD1 PE=1 SV=2
24	Urea transporter 1 OS=Homo sapiens GN=SLC14A1 PE=1 SV=2
25	Ribonuclease 3 OS=Homo sapiens GN=DROSHA PE=1 SV=2
26	Dapper homolog 1 OS=Homo sapiens GN=DACT1 PE=1 SV=2
27	E3 ubiquitin-protein ligase HERC2 OS=Homo sapiens GN=HERC2 PE=1 SV=2
28	Putative heat shock protein HSP 90-beta 2 OS=Homo sapiens GN=HSP90AB2P PE=1 SV=2
29	Histone H2A type 1-A OS=Homo sapiens GN=HIST1H2AA PE=1 SV=3
30	40S ribosomal protein S28 OS=Homo sapiens GN=RPS28 PE=1 SV=1

Table S6 Identified protein list from the protein corona of AuNPs exposed to A2780 cell lysate. The protein with the highest protein score is hit number 1 and so on.

Rh-SiNPs characterization

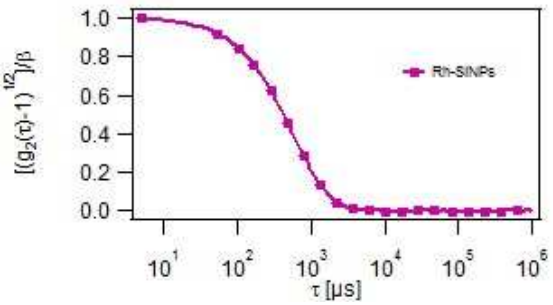

	Rh-SiNPs
D_H	67.2 ± 0.3
PDI	0.188 ± 0.016
ζ-Potential	-31.07 ± 0.5

Figure S1: Dynamic light scattering ACF registered for Rh-SiNPs; summary of Rh-SiNPs main properties: hydrodynamic diameter (D_H), polydispersity (PDI) and surface potential.

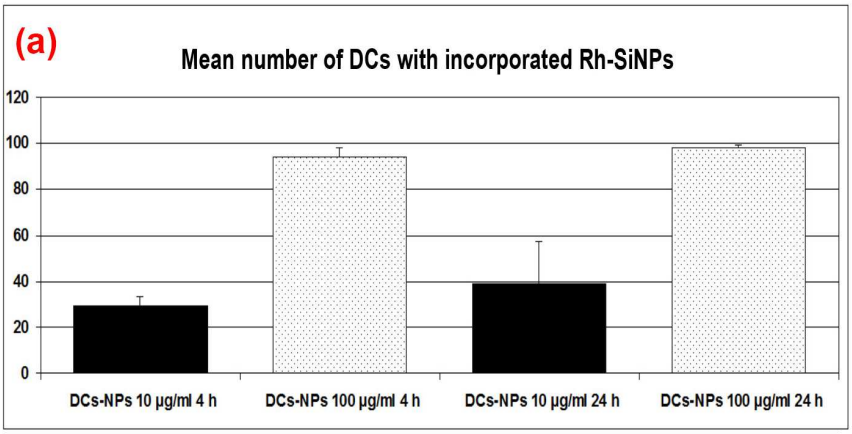

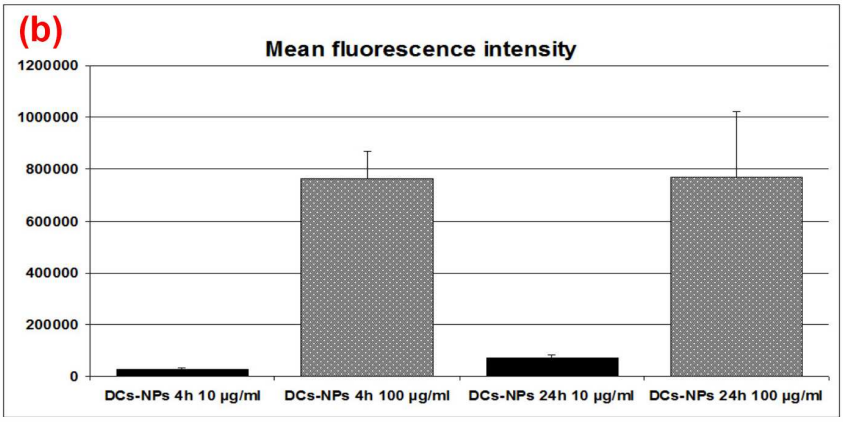

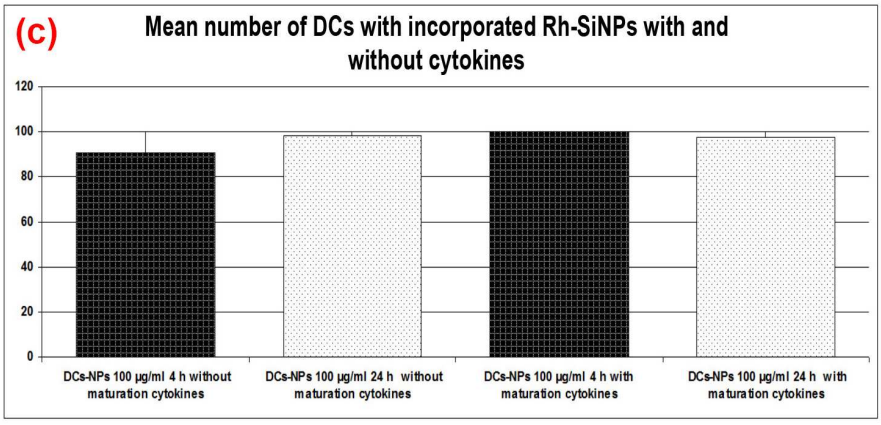

Figure S2 (a) Percentage of DCs with internalized fluorescent silica NPs (10 e 100 µg/ml) after 4 e 24 h of incubation without maturation-inducing cytokines. Mean and standard error of two (10 µg/mL NPs) and four (100 µg/mL) independent experiments. At each time point, the difference between NPs concentrations was significant (*p<0,05), while the difference between time points for each concentration was not significant; (b) Fluorescence intensity of DCs that internalized fluorescent silica NPs (10 e 100 µg/ml) after 4 e 24 h of incubation without maturation-inducing cytokines. Arbitrary units; the mean and standard error were calculated assuming each cell as a sample unit; N = 15~35 depending on experiment. The difference between NPs concentrations was significant (**p<0,01) at 4h, while the different between 4 and 24 h was significant (**p<0,01) for the 10 µg/ml concentration; (c) Percentage of DCs that internalized fluorescent silica NPs (100 µg/ml) after 4 and 24 h of incubation with and without maturation-inducing cytokines; N=2. No significant difference was found.

Viability (%)

	10 µg/ml	25 µg/ml	75 µg/ml	100 µg/ml
SiNPs	91.8 ± 1.5	92 ± 2.2	ND	91.4 ± 1.3
AuNPs	91.7 ± 2.6	ND	94 ± 1.9	93.2 ± 1.6

Table S7 Effect of AuNPs and SiNPs on DC viability (%) assessed by means of flow cytometry. Dead cells were excluded by 7-ADD. Means ± SEM, n=5

Supplementary Materials and Methods

Transmission Electron Microscopy (TEM) of NPs Transmission Electron Microscopy (TEM) images were acquired with a STEM CM12 Philips electron microscope. The nanoparticle samples dispersed in hexane solution were cast onto a carbon-coated copper grid sample holder, followed by evaporation at room temperature.

Dynamic Light Scattering (DLS) DLS experiments were carried out on a Brookhaven Instrument apparatus, New York, USA (BI 9000 AT correlator card and BI 200 SM goniometer). The signal is detected by an EMI 9863B/350 photomultiplier. The light source was the doubled frequency of a Coherent Innova diode pumped Nd-YAG laser, (λ=532 nm, 20 mW), or alternatively a JDS Uniphase He-Ne (λ=633 nm, 5 mW). The laser long term power stability was 0.5%. Self-beating detection was recorded using decahydronaphthalene (thermostated by a water circulating system) as index matching liquid. A temperature probe was inserted in the sample while simultaneously recording autocorrelation functions. Measurements have been performed at 25°C on 0.5 ml samples previously transferred into cylindrical Hellma scattering cells. For each sample at least three separate measurements were performed at the scattering angle θ = 90° corresponding to the scattering vector q. Data analysis has been performed according to standard procedures, and interpreted through a cumulant expansion of the field autocorrelation function, arrested to the second order.

One of the most common methods to fit DLS autocorrelation functions is the Cumulant method, from which in addition to the sum of the exponentials above, more information can be derived about the polydispersity of the system as follows:

$$g_1(q,\tau) = \exp(-\Gamma\tau)[1 + (\mu_2/2!)\tau^2 - (\mu_3/3!)\tau^3 + ...) \quad (1)$$

where $(\mu_2/2!)\tau^2$ is the second order polydispersity index. An alternative method for analyzing the autocorrelation function for highly polydisperse or multimodal system can be achieved through an inverse Laplace transform through the CONTIN algorithm, developed by Provencher[1].

Zeta Potential Zeta potential measurements were carried out using a Zeta Potential Analyzer (Brookhaven Instruments Corporation, Holtsville, NY). Zeta potential values were

obtained from the electrophoretic mobility u, according to Helmholtz-Smoluchowski equation (Eq. 2):

$$\zeta = (\eta/\varepsilon)u \quad (2)$$

with η being the viscosity of the medium and ε the dielectric permittivity of the dispersing medium. The zeta potential values are reported as averages from 5 measurements on each sample.

Circular Dichroism Circular Dichroism measurements were performed on a JASCO J-600 spectropolarimeter, in the 350-190 nm range, using Hellma 1 mm pathlength quartz cuvettes**.**

Fluorescence microscopy To follow the incorporation of fluorescent silica NPs, for each experiment and experimental condition a drop of culture medium containing about 100 unfixed cells was transferred to a microscopic slide, covered with a coverslip, observed in an Axioskop microscope equipped for epifluorescence (Zeiss, Oberkochen, Germany) and captured with an Axio Vision 4 system, consisting of a digital multichannel fluorescence module and dedicated software (Zeiss). The number of unlabelled and that of labelled cells were counted and the percentage of labelled cells per slide was computed. Among labelled cells, the intensity of fluorescence was measured with ImageJ for Windows (NIH, Bethesda, MD): each labelled cell was outlined by hand and the software was used to measure the surface area (in square pixel, pixel size 0.0256 μm^2) and the mean labelling intensity (in arbitrary units, maximum intensity = 255) of the cell. The two measures were multiplied for each other to obtain the total labelling per labelled cell.

Transmission Electron Microscopy (TEM) of DCs Cytocentrifugates were fixed in 2% formaldehyde and 2.5% glutaraldehyde in 0.1 mol/L cacodylate buffer, pH 7.4, osmicated and embedded in epoxy resin. Sections were stained with gadolinium acetate [2] and either lead citrate or bismuth subnitrate [3], and observed in a Jeol JEM 1010 electron microscope (Tokyo, Japan) at 80 kV. Photomicrographs were taken with a digital camera MegaView III (Soft Imaging System, Muenster, Germany) connected with a personal computer (Dell, Round Rock, Texas) with dedicated software (AnalySIS, Soft Imaging System, Muenster, Germany).

Flow cytometry analysis of DC maturation. Dendritic cells incubated with NPs were harvested and stained with following fluorescent monoclonal antibodies to analyze their maturation: phycoerythrin (PE) conjugated CD83, fluorescein isothiocyanate (FITC) conjugated CD80 and allophycocyanin (APC) conjugated CD86 (all from BD Biosciences, San Jose, CA). In order to block Fc-mediated unspecific binding, cells were pre-incubated with 1% FBS in PBS for 30 min at 4°C. 7-AAD was used to recognize dead cells and exclude them from analysis. Isotype-matched antibodies were used as negative controls. Flow cytometry was performed on FACScanto II and data was analyzed with FACs Diva Software (BD Biosciences).

Mixed lymphocyte reaction Lymphocytes were stained with the fluorescent dye CFSE following manufacturer instructions. $2x10^5$ lymphocytes were cultured 5 days in complete medium with $4x10^4$ DCs pre-incubated with NPs. Immature DCs, DCs matured with cytokines and lymphocytes stimulated with 5 µg/ml phytohaemoagglutinin (PHA, Biochrom, Holliston, MA) were used as controls. After 5 days lymphocytes were recovered and stained with the following fluorescent monoclonal antibodies following manufacturer's instructions: PerCP-Cy5.5 conjugated CD3, CD4-PE and CD8-APC (BD Bioscience). Block of Fc-mediated unspecific binding and flow cytometry analysis were performed as above. Isotype-matched antibodies were used as negative controls.

Statistics Quantitative data were expressed as mean ± standard error (SE) and analyzed as appropriate by ANOVA and Student t-test for paired data. Statistical significance was assumed for $P<0,05$.

Mass spectrometry

Solvents, reagents and materials

Water (412091) and acetonitrile (412042), both UHPLC-MS grade, were purchased from Carlo Erba (BP 616, F-27106, Val de Reuil Cedex, France). Methanol LC-MS grade (34966), ammonium hydrogen carbonate (Ambic, 09830), dithiothreitol (DTT, 43815), iodoacetamide (IAA, 57670), formic acid (56302, eluent additive for LC-MS), acetic acid (49199-F, eluent additive for LC-MS) and trifluoroacetic acid (TFA, 40967, eluent additive for LC-MS eluent additive for LC-MS) were purchased from Sigma-Aldrich (St. Louis, MO, USA). Sequencing grade modified trypsin (Tryp, V5111) was purchased from Promega (Madison, WI, USA) and Lys-C Endoproteinase MS-grade from Thermo Scientific (Rockford, IL, USA). The hand-made desalting/purification STop And Go Extraction tips (StageTips) were prepared [4] using C18 Empore Disks (2215) purchased from 3M (MN, USA). Microcon centrifugal filter devices with a nominal cutoff of 10 kDa (MCRPRT010) were purchased from Merck Millipore (Tullagreen, Carrigtwohill Co. Cork, Ireland).

Lysate solution purification from protease inhibitor cocktail

First of all, the protease inhibitor cocktail (P8340, Sigma) was removed from both the lysates: 10 µl of lysate solution, containing 15 µg of lysate, were loaded onto a centrifugal filter device (cut off 10 kDa) together with 490 µl of H_2O, spinned for 20 minutes at 13000 rpm, diluted again to 500 µl with H_2O and spinned for 30 minutes at 13000 rpm; the inverted filters were then spinned at 4000 rpm for 3 minutes thus recovering 30 µl of purified lysate solution.

Protein reduction, alkylation and digestion

The following six solutions were subjected to the reduction, alkylation and digestion protocol in use in our laboratory [5].

Solutions 1) and 2): 30 µl of purified lysate aqueous solution of Hep G2 (or A2780) containing 15 µg of lysate (considering a 100% recovery from the previous centrifugation steps).

Solutions 3), 4), 5), 6): 30 µl of AuNPs (or SiNPs) incubation solution purified from the unbound lysate (Hep G2 or A2780) containing less than 7.5 µg of bound lysate.

The reduction step was performed by adding 1 µl of 0.5 µg/µl DTT aqueous solution to the six samples and incubating for 30 minutes at RT. The alkylation step was performed by adding 1 µl of 2.5 µg/µl IAA aqueous solution to the six samples and incubating for 20 minutes at RT in the dark. The samples were then three-fold diluted with Ambic 50 mM (pH 8.5) to the final volume of 90 µl. A first digestion step was performed by adding 1 µl of 0.4 µg/µl LysC aqueous solution to each sample and incubating for 3 hours at 37°C. A second digestion step was performed by adding 1 µl of 0.5 µg/µl Tryp aqueous solution to the six samples and incubating overnight at 37°C. The digestions were stopped by adding 20 µl of 10% TFA to each sample (final pH value under 3; final sample volume about 110 µl). Digested samples 1) and 2) were directly purified on StageTip while NPs were preventively removed from digested samples 3), 4), 5), 6).

Removal of AuNPs and SiNPs from digested samples

The AuNPs and SiNPs were removed from the peptide mixture coming from samples 3), 4), 5) and 6) [6]:

- 400 µl of CH_3CN were added to the 110 µl of peptide mixture (final volume 510 µl)
- the four samples were centrifuged at 13000 rpm for 5 minutes to pellet the NPs
- in the four Eppendorf it was not possible to see precipitation and it was decided to conservatively withdraw only 450 µl
- this volume was concentrated to less than 100 µl before StageTip purification step.

StageTip purification step and nanoLC-MS/MS analyses

The entire volume of the six digested samples was purified on StageTip[4] following the standard protocol and the eluates were concentrated and reconstituted to 20 µl in 0.5% CH_3COOH [7].
The six peptide mixtures were submitted to nanoLC-MS/MS analysis on an Ultimate 3000 HPLC (Dionex, San Donato Milanese, Milano, Italy) coupled to a LTQ-Orbitrap mass spectrometer (Thermo Fisher, Bremen, Germany). For each solution a volume of 5 µl was directly injected on a self-made nanocolumn packed with an Aeris Peptide XB-C18 phase (75 µm i.d. × 15 cm, 3.6 µm, 100 Å, Phenomenex, Torrance, CA, USA) and eluted at 300 nL/min flow rate. The mobile phase composition was: H_2O/CH_3CN 97/3 with 0.1% HCOOH (phase A) and CH_3CN/H_2O 80/20 with 0.1% HCOOH (phase B). The elution gradient program was: 0 min, 2% B; 40 min, 2% B; 68 min, 15% B; 168 min, 25% B; 228 min, 35% B; 273 min, 50% B; 274 min, 90% B; 288 min, 90% B;

289 min, 2% B; 309 min, 2% B. Mass spectra were acquired in positive ion mode, setting the spray voltage at 1.8 kV, the capillary voltage and temperature at 45 V and 200 °C, respectively, and the tube lens at 130 V. Data were acquired in data dependent mode with dynamic exclusion enabled (repeat count 2, repeat duration 15 s, and exclusion duration 30 s); survey MS scans were recorded in the Orbitrap analyzer in the mass range of 300–2000 m/z at a 15,000 nominal resolution at m/z = 400; then up to five of the most intense ions in each full MS scan were fragmented (isolation width 3 m/z, normalized collision energy 30) and analyzed in the IT analyzer. Monocharged ions did not trigger MS/MS experiments.

Data processing and analysis

The six raw files were analyzed using Mascot 2.4 search engine (Matrix Science Ltd., London, UK). The database used was SwissProt (version March 15, 2015) and the taxonomy was restricted to *homo sapiens*. The experimental mass values were monoisotopic. Trypsin digestion was assumed. Searches were performed allowing: (i) up to two missed cleavage sites, (ii) 10 ppm of tolerance for the monoisotopic precursor ion and 0.8 mass units for monoisotopic fragment ions, (iii) carbamidomethylation of cysteine and oxidation of methionine as variable modifications. A target-decoy search was used: a false discovery rate (FDR) of 1% was imposed and the criterion used to accept protein identification included probabilistic score sorted by the software. Output files were summarized at the protein level to include one protein (the best identified protein in the protein family present in the hit) per hit.

Bibliography

[1] Provencher SW. CONTIN: A general purpose constrained regularization program for inverting noisy linear algebraic and integral equations. *Computer Physics Communications* 27 (3), 229–242 (1982).

[2] Nakakoshi M, Nishioka H, Katayama E. New versatile staining reagents for biological transmission electron microscopy that substitute for uranyl acetate. *J Electron Microsc* 60 (6), 401-407 (2011).

[3] Riva A. A simple and rapid staining method for enhancing the contrast of tissues previously treated with uranyl acetate. *Journal of Microscopy* 19 (1), 105-108 (1974).

[4] Rappsilber J, Ishihama Y, Mann M. Stop and go extraction tips for matrix-assisted laser desorption/ionization, nanoelectrospray, and LC/MS sample pretreatment in proteomics. *Anal. Chem.* 75, 663-670 (2003).

[5] Iovinella I, Caputo B, Michelucci E, Dani FR, Della Torre A. Candidate biomarkers for mosquito age-grading identified by label-free quantitative analysis of protein expression in Aedes albopictus females. *J. Proteomics* 128, 272-279 (2015).

[6] Arvizo RR, Giri K, Moyano D, Miranda OR, Madden B, McCormick DJ, Bhattacharya R, Rotello VM, Kocher JP, Mukherjee P. Identifying new therapeutic targets via modulation of protein corona formation by engineered nanoparticles. *PLoS ONE* 7, 1-8 (2012).

[7] Rappsilber J, Mann M, Ishihama Y. Protocol for micro-purification, enrichment, pre-fractionation and storage of peptides for proteomics using StageTips. *Nat. Protoc.* 2, 1896-1906 (2007).